Ministry of Education and Science of Ukraine
Ternopil Ivan Puluj National Technical University

Faculty of Computer Information Systems and Software Engineering
(full name of faculty)
Computer Science Department
(full name of department)

QUALIFYING PAPER

For the degree of

Master's thesis
(degree name)

topic: Travolution is a built-in road safety system for passenger cars

Submitted by: fourth year student VI , group ICAm-62
specialty 124 "System Analisys"
(code and name of specialty)

(signature) Tay Efoe Ruben (surname and initials)

Supervisor (signature) Ihor Baran (surname and initials)

Standards verified by (signature) Oleksandr Matsiuk (surname and initials)

Head of Department (signature) Ihor Bodnarchuk (surname and initials)

Reviewer (signature) (surname and initials)

Ternopil
2022

Ministry of Education and Science of Ukraine
Ternopil Ivan Puluj National Technical University

Faculty Faculty of Computer Information Systems and Software Engineering
(full name of faculty)

Department Computer Science Department
(full name of department)

APPROVED BY
Head of Department
_____ Ihor Bodnarchuk
(signature) (surname and initial0073)
«____» _____ 2022 p.

ASSIGNMENT
for QUALIFYING PAPER

for the degree of Master's thesis
(degree name)

specialty 124 "System Analisys"
(шифр і назва спеціальності)

student Tay Efoe Ruben
(code and name of the specialty)

1. Paper topic Travolution is a built-in road safety system for passenger cars

Paper supervisor Ph.D., Assoc. Prof Ihor Baran
(surname, name, patronymic, scientific degree, academic rank)

Approved by university order as of «_22_» _11____ 2022 № _*4/7-951*_____

2. Student's paper submission deadline 22.12.2022

3. Initial data for the paper Technical requirements for system

4. Paper contents (list of issues to be developed)
   1. RESEARCH OF VEHICLE SECURITY SYSTEMS
   2. RESEARCH OF ELECTROMECHANICAL SYSTEMS OF ELECTRIC VEHICLES
   3. DEVELOPMENT OF AN ELECTRIC VEHICLE SAFETY SYSTEM AGAINST A SIDE COLLISION
   4. OCCUPATIONAL HEALTH AND EMERGENCY SAFETY

5. List of graphic material (with exact number of required drawings, slides)
   1. Title slide
   2. Actuality
   3. Purpose of work
   4. Main part
   5. Conclusion

6. Advisors of paper chapters

Chapter	Advisor's surname, initials and position	Signature, date	
		assignment was given by	assignment was received by
OCCUPATIONAL HEALTH			
AND EMERGENCY SAFETY			

7. Date of receiving the assignment _____

TIME SCHEDULE

LN	Paper stages	Paper stages deadlines	**Notes**

Student _____ Tay Efoe Ruben
(signature) (surname and initials)

Paper supervisor _____ Ihor Baran
(signature) (surname and initials)

ANNOTATION

Travolution is a built-in road safety system for passenger cars // Qualification work of the educational level "Master" // Tay Efoe Ruben // Ternopil National Technical University named after Ivan Pulyuy, Faculty of Computer Information Systems and Software Engineering, Department of Computer Science, ICAm-62 group // Ternopil, 2022 // P. ___, fig. - ___, tables - ___, chair. - ___, annexes - ___, references. - ___.

Key words: information system, electric car, safety system, side collision, machine vision, electro-mechanical systems.

The object of research is the processes taking place in the active electropneumatic suspension of an electric car to reduce the consequences of an accident in the event of a side collision.

The purpose of the research is to increase the passive safety of the electric vehicle account of the research and development of the side impact safety system.

Research method – research and development of electrical systems and complexes of electric vehicles.

The subject of the study is the safety system of an electric car against side impact collision.

The master's thesis solves an actual problem related to increasing the passive safety of an electric vehicle due to research and development of a side collision safety system.

LIST OF SYMBOLS, SYMBOLS, UNITS, ABBREVIATIONS AND TERMS

IS - information system

EC - electric car,

SS - safety system

SC - side collision

MV - machine vision,

EMC - electro-mechanical systems.

CONTENT

INTRODUCTION

The master's thesis solves an urgent problem related to increasing the passive safety of an electric vehicle, as rule, through the research and development of a side collision safety system. The relevance of this study is that it allows for a detailed analysis and research of all modern advanced technologies of safety systems, as we see, used in the creation electric cars of various brands, on the basis, usually, of which to develop conceptual and schematic solutions for the protection, as we see, of the driver and passengers from a side collision. The main scientific and practical result, usually, of completing the master's thesis consists in confirming qualifications in the process of mastering theoretical and practical skills in the analysis, diagnosis, repair and maintenance of electromechanical safety systems of electric, as rule, vehicles. When start the research, the skills of processing technical literature, practical skills of conducting analysis of electromechanical safety systems (SS) of electric vehicles are consolidated. The practical skills of conducting diagnostics of electromechanical SS of electric vehicles, which were acquired during training and practical training, allow you to learn how to properly submit material, carry out diagnostics, repair and adjustment of various systems of electric vehicles, draw appropriate conclusions and make suggestions for development and repair.

As a result of the research:

- studies of the safety systems of such electric cars as Tesla Model 3 and AUDI E-TRONE were carried out, namely, general data about electric cars were determined, active and passive safety systems were studied, battery protection measures during a collision were studied, etc.;

- studies of car safety systems against side collisions were carried out, usualy, the features of the main SS for the Tesla Model 3 and AUDI E-TRONE, such as the response, usually, of the electro-pneumatic suspension system during a collision;

- development of an electric vehicle safety system against side impact, which is based on the use of electromagnetic processes occurring in the active electropneumatic suspension of an electric vehicle to lower influence the consequences of an accident in the event of a side impact;

- to consider issues of occupational health and safety in emergency situations during maintenance and repair of safety systems and other electromechanical systems and complexes of electric vehicles, performed engineering calculations related to occupational health and safety;

- the calculation of competitiveness was carried out and the assessment of the economic efficiency for the our solutions was carried out;

- based on the results uor research, the conclusions was determined.

1 RESEARCH OF VEHICLE SECURITY SYSTEMS

1.1 Car security systems

The following basic requirements are made, as we can see, to the safety of the car: it must have such technical qualities that will help the driver confidently and reliably manage them with minimal power, well guided in different situations, will ensure the life and passengers will be preserved in the accident [1]. The car should be, as rule, designed to reduce the likelihood of a road accident and, as rule, to provide the driver with a critical position to find the right solution. This is the SS of the car. Thus, everything that can prevent the accident belongs to active safety.

The most, usually, important signs of active SS are:

- the motion safety, which is determined by the balance of the suspension, its rigidity and in rotation stability, the accuracy, as rule, of the steering, the brake system power, the inhibition stability;

- the driver's conditionas, as you can see, safety, which load on the driver, caused by the oscillations of the seat, body, usually, the noise of the running part and, as rule, the engine, as well as the climatic environment. All these factors should be minimally affected by the driver, as normally, to reduce its load;

- the safety of perception, which depends on the outdoor lighting of the car, the examination, which is determined by the minimum number of so -called "dead zones" that fall out of view of the driver;

- control safety related to the logical arrangement, usually, of controls, such as light switch, wiper lever, air conditioning, radio, etc. All items should be arranged in such a way as to have good access from the driver's place.

Active SS prevent dangerous situations, regardless of whether they are external or occurring through the driver and plus are a consequence of its

inattention or fatigue. The active SS of the car is aimed at preventing the accident. To do this, the car is equipped with additional systems that help the driver and sometimes operate regardless of it. The active safety of the transopt device is, first of all, to ensuring the reliable operation of all elements and systems of him, the ability to confidently and with comfort to drive a vehicle, to ensure traction and brake dynamics of the car in accordance with the road conditions and the road situation, as well as to the psychophysiological features of the driver .

The desire to increase active safety, it is almost impossible, as rule, to completely exclude a road accident. Therefore, the car should be such that, as rule, in the event of a road accident, when the passengers and driver become only passive participants of events and no longer have time or the ability to interfere with the way and make, usually, the severity of the consequences minimal.

All measures and systems aimed at this purpose, usually, are considered to be passive SS of the transport device. The elements of passive safety have realized possibilities of preserving the lives of traffic participants, the driver - car - road environment (VADS) should provide the necessary level of post -avarium safety. The fact, as we see, is that many accidents are the fire of a transopt device, the main sources of which include the fuel tank, high voltage recharge and other parts of the system power management [2].

The car SS are responsible to driver, passengers in the transpot device and other road user are not injured after the accident. Passive safety include the systems, elements of the transpot device that are included in the work directly at the time, as we see, of the accident. Their main task is to save the lives of passengers and to minimize injuries. The term "passive safety" itself indicates that it does not distract the emergency, is in a passive anticipation to mitigate its consequences.

1.2 Active Safety Systems

With the advent of computers, transpot devices began to install electronic security systems. Vehicles have learned to control the roads through wireless infrared sensors, lasers, leaders or cameras. Such electronic systems warn of possible contact. For example, they detect rapidly approaching objects (suddenly stopped deer, transport in front of a traffic light or pedestrian) will tell if the car drove out of its lane or the driver fell asleep at the wheel. Examples of active SS, transpot devices are shown in Figure 1.1 [3].

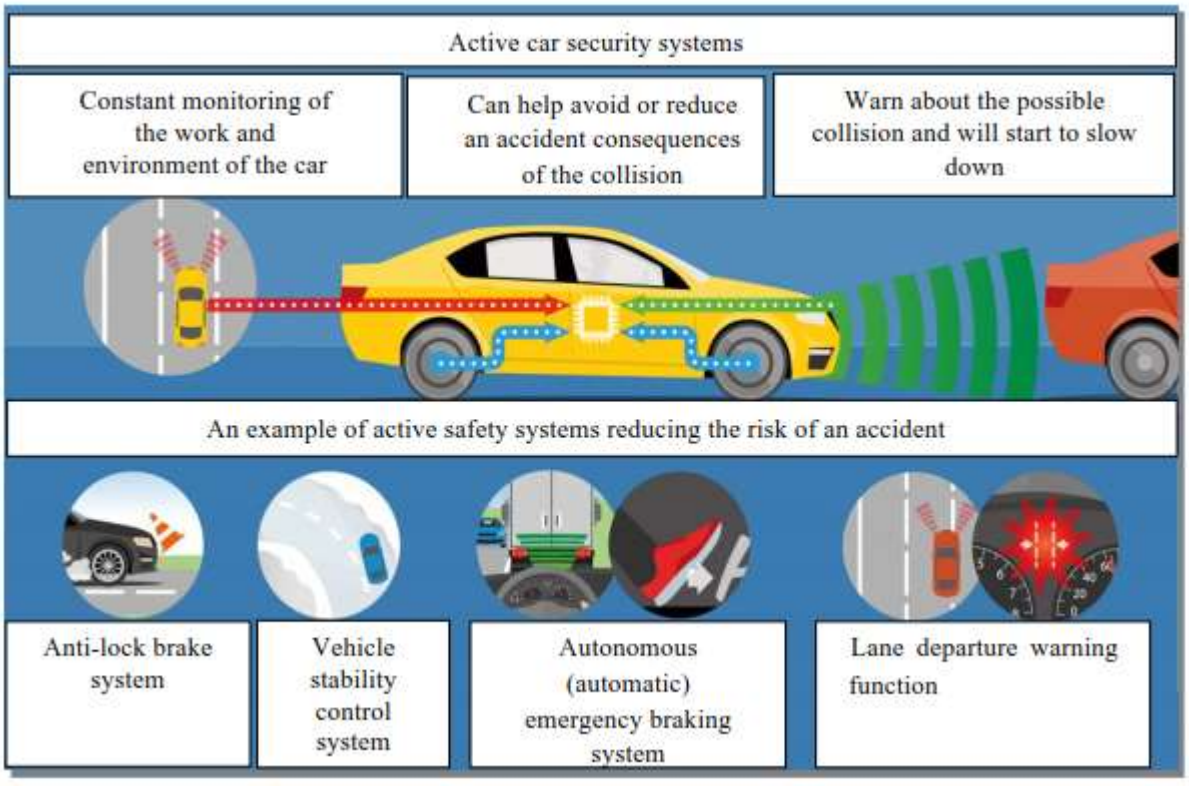

Figure 1.1 - An example of active security systems

If the car locks a possible collision, the warning lights and the signals will notify the car driver, and computer controller will start to furnish to give a chance

him to react and stop in a timely manner. The seat belts, as we see, will automatically stretch, the heads will move forward to involve prevent injury to the neck, back and spine, and the seat will take a vertical position.

Modern systems electronic type of the transpot device have several cameras. For example, four chambers (circular survey cameras) monitor the road situation, and the heel installed in the salon and analyzes the driver's face to care for the situation on the road. If CPU control system that comes, as we see, from the cameras believes that the accident will happen before the driver is able to respond, the car will brake on its own. Even the cameras recognize the driver behind the wheel and signal it to awaken, including the emergency system, make a forced stop without human help.

We will conduct research of some active SS of modern transport device.

Night vision systems.

The night vision system give possibilities people regardless of the level of light in the dark, and colors and reflects obstacles on the display. This improves the visibility of pedestrians, regardless of the color of their clothes. Usually, the risk of road accidents is significantly reduced. Illustration of night vision system and how it work are given in Figure 1.2 [4].

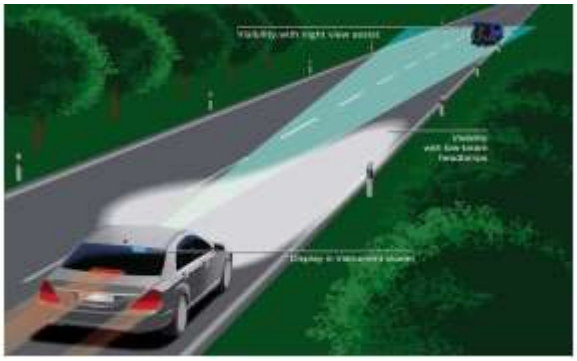

Figure 1.2 - Illustration of the Night Vision System

This illustration (see Figure 1.2) shows, as we can see, the advantages of the carman using a night vision system. The pedestrian moving on the road is just beginning to appear in the field of view when looking through the windshield.

However, on the screen of the night vision system, it is already noticeable in full height. The pedestrian figure is clearly, usually, distinguished by a light color on the surrounding background and to prevent the danger of collision is surrounded by a red frame. The early detection of a pedestrian gives the carman more time to respond properly to a dangerous situation. The night vision system is associated with systems that slows the acceleration of the transport device from 0 to 100 km/h at night. The acceleration would take 3.5 s in the afternoon, then at night the car will only drive in 15 seconds.

Deviation system of the selected strip.

The system of deviation from the selected lane (LDWS) tracks the movement of the transport devices in its lane and will give a signal or torn the car if the driver starts to slowly leave it into the ditch. Models detecting blind zones control the situation with cameras and infrared, as rule, sensors installed in lateral mirrors. The sensors track the passing transport on the road that does not fall into the view of carmans. When a foreign car enters the area of a blind spot, CPU system start to send signals to the carman with a tinter or blinking diodes on mirrors, Figure 1.3.

Figure 1.3 - An example operation control zones for CPU control system

Stability course electronic system (ECSS).

The ECSS provides the driver with the best control of the movement of the transport device, ensuring that it, usually, moves in the same direction where is rotated steering wheel.

From a technical point of view, the ECSS can be considered as an extended version of the anticlocking brakes system (ABS). Many nodes are combined with this system, but in addition, as ruke, to its components, the sensor of steering type and the axlerometer of the lateral accelerations, which are track on the process of real rotation of the car, Figure 1.4 [5].

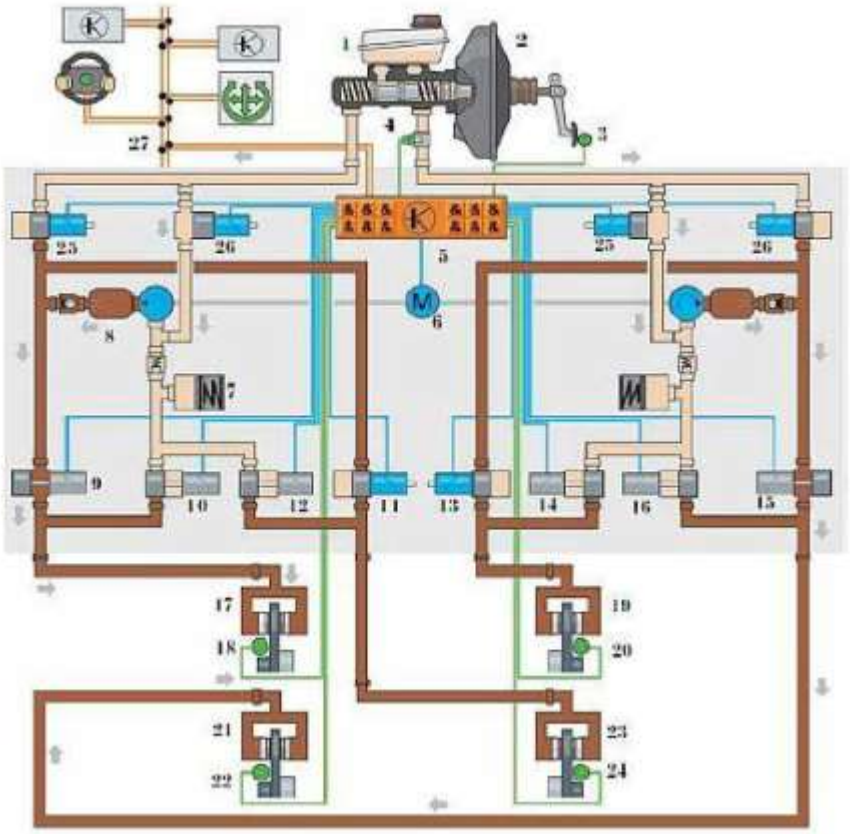

Figure 1.4 - УICC: 1 - compensatory tank; 2 - vacuum brake amplifier; 3 - brake pedal position sensor; 4 - pressure sensor in the braking system; 5 - control unit; 6 - reverse pump; 7 - pressure battery; 8 - the damping camera; 9 - inlet valve of the front left brake mechanism; 10 - outlet valve of the front left brake mechanism; 11 - inlet valve of the carman of the rear right mechanism of brake; 12 - the outlet valve of the rear right brake mechanism; 13 - inlet valve of the front

right brake mechanism; 14 - exhaust valve of the front right brake mechanism; 15 - inlet valve of the rear left brake mechanism; 16 - outlet valve of the rear left brake mechanism; 17 - front left brake cylinder; 18 - the sensor rotation speed of wheel front left; 19 - anterior right brake cylinder; 20 - the rotation sensor speed of wheel front right; 21 - rear left brake cylinder; 22 - the rear left wheel rotation sensor; 23 - rear right brake cylinder; 24 - the speed rotation sensor of rear wheel right; 25 - valve of switching; 26 – valve of pressure high; 27 - data exchange tire.

Determining the onset of the emergency is carried out by comparing the driver's actions and the parameters of the car. When driver's actions (desired motion parameters) differ from the actual parameters of the car, the ESC system is included. The main sensors of the electronic course stability system are shown in table 1.1.

Table 1.1

The main type sensors of the ECSS

Functional purpose	Sensor
Used in an assessment of actions driver	The angle of rotation of the steering wheel
	The pressure sensor in the brake system
	Stop swap
Used in assessing the actual car traffic parameters	Angular speed sensors
	Longitudinal acceleration sensor
	The transverse acceleration sensor
	The speed of turning the car
	The pressure sensor in the brake system

Cruise adaptive system for control (ACC).

The ACC system is shown in Figure 1.5.

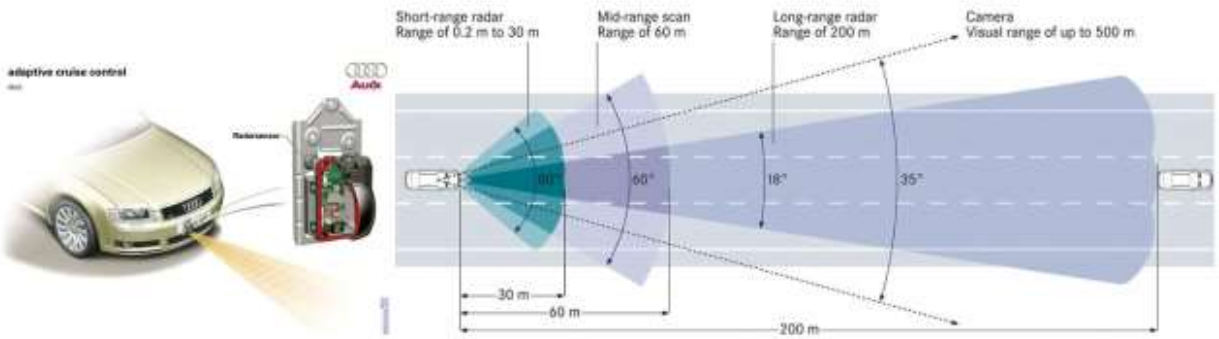

Figure 1.5 - A system of adaptive cruise control

1.3 Safety Passive System

The PSS main elements are:

- airbags;
- seat belts;
- soft elements of the salon or disinfection;
- zones of deformation of the body;
- folding steering column;
- traumatic pedal knot;
- seat headrests;
- safe glass;
- safety arcs;
- enhanced front roof racks;
- Transverse bars in the door, etc.

The airbags went the way from simple front to the lateral curtains that shoot at an accident, for the barriers from the broken glass of passengers. The latest trend was the installation of car airbags for the pedestrian. The scheme of the layout of the side pillow and the scheme of layout of the pedestrian pillow is shown in Figure 1.6.

Figure 1.6 - Scheme of layout of side pillow and pedestrian pillow

We will conduct research SUPPLEMENTARY RESTRAINT SYSTEM (SRS), which is designed to ensure driver's safety and passengers in contact with static or moving objects.

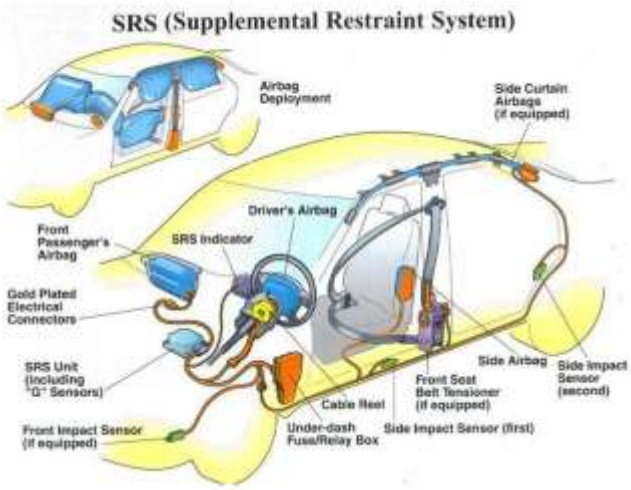

Figure 1.7 - Supplementary Restraint PSS

The this system main task of is to minimize injuries and their severity for vehicle passengers in an accident. The pillows and straps tensilers and straps that protect the person from the blow to the windshield or other objects in the cabin are immediately triggered. This system to work, is supplied a pulse signal.

The airbags are installed and programmed in such a way that they only work with front or side blows. In cases where the blow falls behind, neither the belts nor the pillows work. The additional safety system will not be activated by low speeds and if contact with unjust objects. The efficiency of the additional security system

is engaged in microprocessors in the impact sensor block. If the system is damaged, the malfunction will be indicated on the dashboard, and the characteristics of the damage will be recorded and stored in the memory of the system. After identifying the problem, it is recommended that you visit a service center immediately, where professionals will eliminate damage and restore the security system.

It is SRS and a system that will really help save a person's life and avoid serious injuries in the event of a road accident. It is for this reason that you cannot ignore the malfunction of the system. And it is very important to follow simple recommendations for using the system. The main one is to prevent SRS overheating more than ninety degrees. At higher temperatures, the system can fail. After ten years of operation of the vehicle, all electronic systems and security devices should be diagnosed [6, 7].

2 RESEARCH OF ELECTROMECHANICAL SYSTEMS OF ELECTRIC VEHICLES

2.1 Tesla Model S electromechanical systems

Tesla Model S P100D electric drive. We will conduct an analysis of the layout of the Tesla Model S P100D electric drive, which is made as a five-door fastback with an all-aluminum body. In the P100D marking, the first letter P is the Perfomans version of the car, the letter D means 4x4 drive (Dual Motor), i.e. one electric motor for each axle. The layout diagram of the P100D transmission and the front Unit Drive are shown in Figure 2.1 [8].

Figure 2.1 – Tesla Model S P100D transmission layout diagram, front and rear Drive Unit.

The electric motors mechanical characteristics of of Tesla Model S are presented in Figure 2.2. The reducer and inverter with the protective cover removed is shown in Figure 2.3.

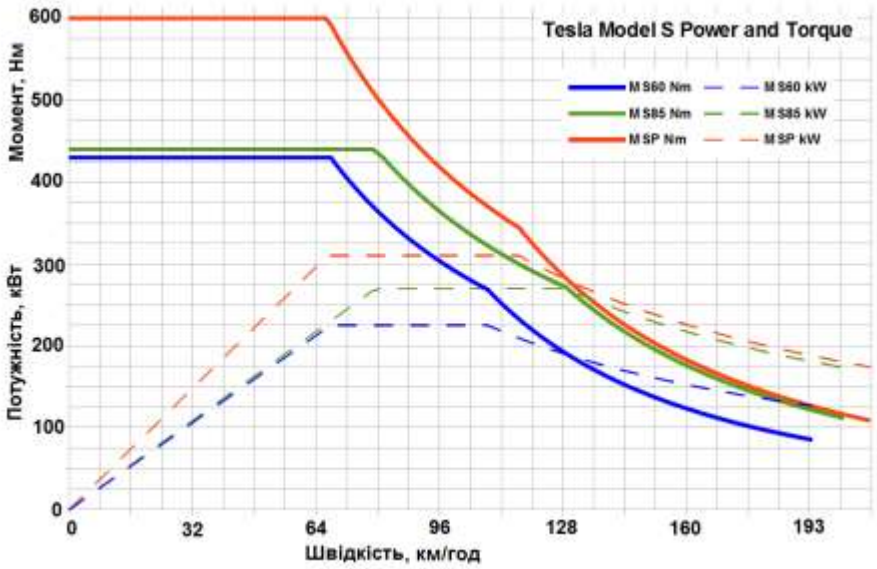

Figure 2.2 – Mechanical characteristics of electric motors of Tesla Model S cars

The voltage converter contains two digital signal processors (DSP) on the control board. The main DSP controls the engine, monitors the performance of the drive system and processes the driver's requests. The second DSP is a safety monitor that can stop torque generation if motor currents, speed, or accelerator pedal conditions indicate that the primary DSP is malfunctioning. The programmable gate array (FPGA) on the control board manages various security and protection schemes at the hardware level.

The engine, gearbox and drive converter have a common liquid cooling system. The coolant enters the motor side of the drive and passes through the gearbox and drive inverter through a series of internal passages, Figure 2.4.

We will conduct a study of the structure and principle of operation of an asynchronous motor (AD), Figure 2.5 [10].

Three-phase ACs are the most widely used in industry [11]. The principle of AD operation is based on the use of a magnetic field, which rotates The speed of rotation of the rotor differs from the synchronous speed of rotation of the magnetic field by a small amount. The difference between the rotation frequency of the stator field and the rotation frequency of the rotor is called the slip frequency n_s.

Figure 2.3 – Reducer and inverter: 1 – circular transmission; 2 – gearbox housing; 3 – differential gears; 4 – reducer of the intermediate shaft; 5 – oil pump; 6 – cardan shaft seal; 7 – differential bearing

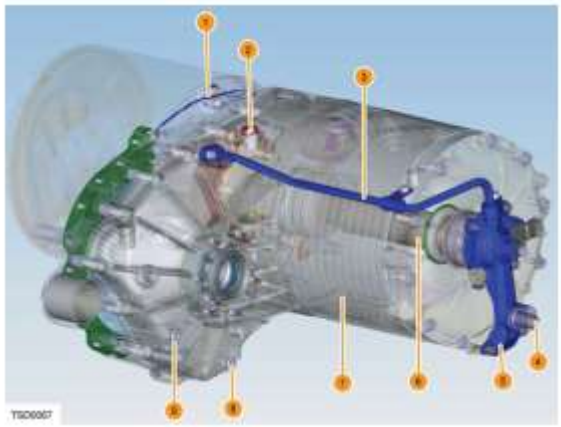

Figure 2.4 - Tesla Model S electric drive cooling system: 1 – air removal; 2 – breather; 3 – coolant pipe; 4 – coolant inlet; 5 - coolant collector; 6 – rotary cooler; 7 – stator cooling jacket; 8 – plug for draining transmission oil; 9 - transmission oil filling / transmission oil level plug.

This is the frequency of rotation at which the field crosses the conductors of the rotor winding:

$$n_S = n - n1, \tag{2.1}$$

where n is the rotation speed of the stator magnetic field;

n1 - speed of rotation of the rotor.

The ratio of the slip frequency to the field rotation frequency is called slip [12].

$$s = \frac{n - n1}{n}, \tag{2.2}$$

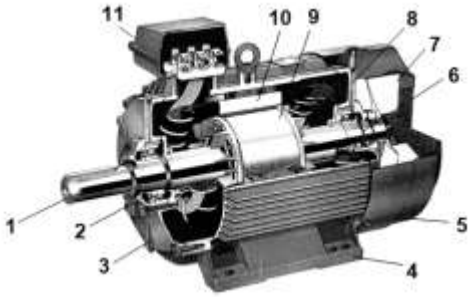

Figure 2.5 - Structure of an asynchronous motor: 1 – shaft; 2, 6 – bearings; 3, 8 – bearing shields; 4 – paws; 5 – fan casing; 7– fan blade; 9 – short-circuited rotor; 10 – stator; 11 - terminal box.

Sometimes slippage is measured in percent, then a factor of 100% is entered in formula (2.2). With of a counter torque on the motor shaft, the slip increases, which causes an increase in the conductors in the current of the rotor winding, and therefore the electromagnetic torque.

Thus, the slip of an induction motor, and therefore the frequency of rotation of the rotor, depend on the load, with the increase of which the frequency of rotation decreases (slip increases). In the general case, the slip of an induction motor can vary in the range from zero (idle mode) to one (starting the motor). Slip and rotation frequency corresponding to the nominal load are called nominal. The nominal slip of induction motors in general use is generally between 1% and 8%, with larger values of slip corresponding to lower power motors.

.

After transforming the (2.2), we obtain the expression of the rotation frequency for the rotor.

$$n1 = n(1 - s), \tag{2.3}$$

Let's represent the rotating magnetic field AD in the form of a field of two magnetic poles rotating in space with a synchronous angular velocity

$$\omega = \frac{2 \cdot \pi \cdot n}{60}, \tag{2.4}$$

Currents are induced in the conductors of the closed rotor winding during rotation. Electromagnetic forces Fem arise from the interaction of the pole field with the rotor currents, under the influence of which the rotor will rotate in the same direction as the magnet poles, only with a slightly lower angular speed

$$\omega 1 = \frac{2 \cdot \pi \cdot n1}{60}, \tag{2.5}$$

The rotation frequency is Hz

$$f = \frac{\omega}{2 \cdot \pi}, \tag{2.6}$$

Then formula (2.3) taking into account formulas (2.4) and (2.6) takes the form:

$$n1 = \frac{60 \cdot f}{p}(1 - s), \tag{2.7}$$

where p is the number of motor pole pairs.

If the slip of a two-pole asynchronous motor connected to the network with a frequency of f1=50 Hz is 7%, then the rotor speed n1 = 60 50 (1 - 0.07) / 1 = 2790 rpm.

The AD rotor winding is not electrically connected to the stator winding. The energy supplied from the network to the stator winding is transmitted to the rotor due to magnetic field. In this respect, an induction motor resembles a transformer, in which the stator winding is the primary winding, and the rotor winding is the secondary.

The difference between an motor asynchronous and a transformer is that the EMF in the windings of the transformer is induced by a pulsating – which changes in time by the magnetic flux, and the EMF in the windings of an asynchronous motor – by a rotating flux, constant in magnitude, but changing its direction in space. But is the same the effect in both cases - the flux grafting between the windings changes over time. Unlike a transformer, the secondary winding of an motor asynchronous - the winding rotor rotates in space [13], [14].

2.2 Tesla Model S power supply system.

The design of the power supply system and the high-voltage circuit of the Tesla Model S electric car is shown in Figure 2.6 [15].

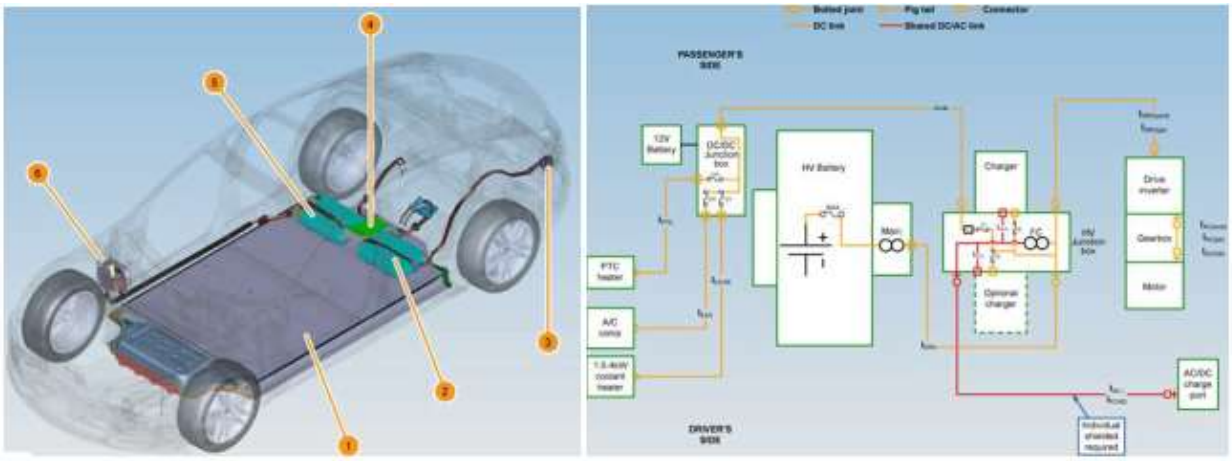

Figure 2.6 - Power system supply design: 1 – 12 V battery; 2 – on-board charger (10 kW); 3 – charging port; 4 – distribution box; 5 – the main charger; 6 - voltage converter.

We will conduct a the features of study of of the systems power in modifications various of the Tesla Model S, which differ not only in battery capacity.

The she was equipped with two batteries types: have a capacity of 40 kWh with 8 sections, which was created on the basis of the Toyota RAV4 EV battery, and A 60 kWh battery that had 12 cells and was programmed to charge up to 40 kWh.

But Tesla Model S 40 was not popular, so their production was soon completed. The Tesla Model S60 battery consisted of 12 or 16 sections. The 12-section battery was installed on the Model S40, the 16-section battery received the designation "NEW" and was radically modified. The 70/75 kWh battery was installed on the Model S60 (S60D), it was also installed on the S70 (S70D) and S75 (S75D), but with enhanced features.

The 60 kWh battery for the 60th model was distinguished by the absence of batteries, for the 70s Model S all 16 sections were completely filled with batteries, due to which the total battery capacity was increased. The Tesla Model S 85, 90 and 100 kWh battery consists of 16 sections. Each cell consists of 444 batteries and has its own BMS board that manages the balancing of all cells. The most popular battery comes from the Tesla Model S 85 (85 kWh), containing 7,104 18650 batteries. In 2015, Panasonic changed the anode design, increasing the battery capacity by about 6%, allowing the battery packs to store up to 90 kWh of energy.

As a result, a 90 kWh battery differs from an 85 kWh battery not only in capacity:

- a Panasonic 18650 battery with an energy capacity of 85 kWh weighs 46 g, and a 90 kWh battery weighs 48.5 g;

- current output in the battery 85 kWh is 10 C, the 90 kWh battery is 25 C (for this reason, the Ludicrous mode is available only in the Model S 90 and 100, because the technical capabilities allow to give the car more lively dynamics);

To further improve battery efficiency and lower costs, Tesla built a large battery factory in Sparks, Nevada, called Gigafactory 1. The factory produces a

new battery design called the 2170. It is 21 mm in diameter and 70 mm in height (see Figure 2.7).

Figure 2.7 - Comparison of 2170 and 18650 batteries

Let's calculate the battery discharge current. To make the calculation, we will decide on the initial data. Accumulators are connected in parallel in groups of 74 pcs. When connected in parallel, the voltage of the group is equal to the voltage of each of the elements (4.2 V), and the capacity of the group is equal to the sum of the capacities of the elements (250 A·h). Next, six groups are connected sequentially into a module. At the same time, the voltage of the module is summed up from the voltages of the groups and is equal to approximately 25 V (4.2 V is multiplied by 6 groups). The capacity remains 250 A·h. Finally, the modules are connected in series in the battery. In total, the battery contains 16 modules (a total of 96 groups). At the same time, the voltage of all modules is summed up and is 400 V as a result (16 modules of 25 V each).

Let's assume that the asynchronous motor for this battery is load of 310 kW. Because

$$P = U \cdot I, \tag{2.8}$$

where P is power;

U – voltage;

I is the current.

In the nominal mode at a voltage of 400 V in the circuit current, A.

$$I = \frac{P}{U} = \frac{310000}{400} = 775. \quad (2.9)$$

But current flows through the parallel connection of 74 batteries. According to first law of Kirchhoff's

$$I = I_1 + I_2 + ... + I_n, \quad (2.10)$$

$$I_n = I / n = 775/74 = 10.5 \quad (2.11)$$

According to data initial, group of batteries capacity are 250 A·h, one battery capacity are 3.38 Ah. The Panasonic 18650 output current battery is 10C, current maximum through battery 33.8 A. Thus, the current obtained from the calculation does not exceed through the battery current maximum. The battery will work reliably at maximum load.

We will build a mathematical model based on a substitution scheme to determine the discharge characteristics of a lithium-ion battery by calculation. The output parameter, as we see, of the mathematical model of accumulators or batteries is the discharge voltage U, and parameter input is the discharge duration p. A typical discharge characteristic of a lithium-ion battery can be divided into three sections:

- two nonlinear sections of initial and final polarization (sections 1 and 3 in Figure 2.8, respectively);

- an almost linear decrease in voltage during discharge (section 2 in Figure 2.8) [9].

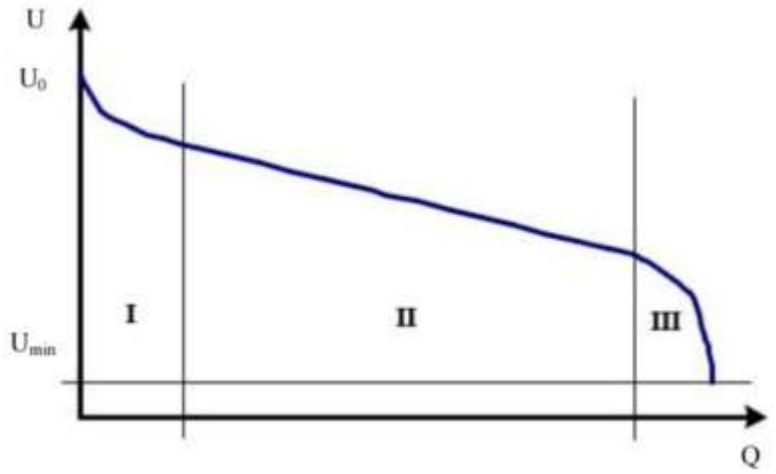

Figure 2.8 – Typical discharge characteristics of a lithium-ion battery

When problem solve, it makes sense to consider the adequacy of the description for each site characteristics. Voltage of discharge a battery of lithium-ion type by current discharge I are mainly affected. In this case mathematical model specific parameters include the ranges of parameters describing the characteristics of batteries and state parameters: initial voltage U_0, internal resistance r_0, initial charge θ_0.

To construct the equations connecting the mathematical model parameters, equivalent electrical substitution circuits were used, which represent active and reactive elements connected in a certain way, each of which simulates a certain parameter of the studied battery. For convenient analysis and analytical representation, the selected replacement scheme into four sections was divided, Figure 2.9.

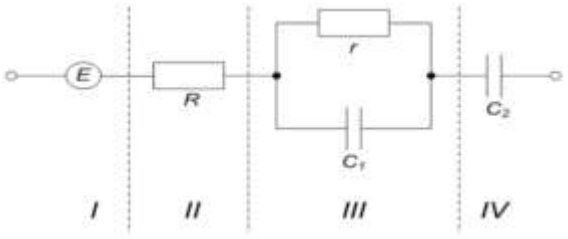

Figure 2.9 – Electrochemical battery replacement scheme

The first section consists of an element representing a source of ideal EMF, the voltage of which is equal to U1 = E. The second section is represented by a resistor R, which describes the resistive part in the operation of the battery. Voltage drop on this element

$$U_2 = R \cdot I\,. \tag{2.12}$$

The third part of the battery replacement circuit is capacitor C1 with a discharge of electricity on resistor r. This section describes the transient processes occurring in the battery when it is switched on for discharge. When passing through the substitution circuit of the constant discharge current I, the equation describing in the section processes has the form

$$U_3 = -b \cdot \left(1 - e^{-\frac{I \cdot t}{C_1 \cdot b}}\right), \tag{2.13}$$

where b is a constant coefficient; t – discharge time, p.

The fourth section of the substitution scheme are represented by capacitor C2, which have discharge process corresponds. When passing through the circuit of a constant discharge current, the processes describing equation in the block has next form

$$U_4 = \frac{Q}{C_2^0} \cdot \left(\ln\left(-Q + I \cdot t\right) - \ln\left(-Q\right)\right), \tag{2.14}$$

where C_2^0 is the coefficient initial capacity corresponding for the torus capacitor C_2;

Q is battery capacity, which able to give when discharged, A·s.

All scheme sections of the substitution are in series connected, so the voltage at the output of the substitution scheme will be determined by their algebraic sum. Thus, the dependence of voltage on time and current for discharge has the following form

$$U = E - R \cdot I + b \cdot \left(e^{\frac{I \cdot t}{C_1 \cdot b}} - 1 \right) + \frac{Q}{C_2^0} \cdot \left(\ln\left(-Q + I \cdot t\right) - \ln\left(-Q\right) \right). \quad (2.15)$$

When forming a mathematical model, it need keep in mind that battery could already release some capacity q part before testing start, then, the characteristic discharge in the next form can be presented:

$$U = E - R \cdot I + b \cdot \left(e^{\frac{q + I \cdot t}{C_1 \cdot b}} - 1 \right) + \frac{Q}{C_2^0} \cdot \left(\ln\left(-Q + q + I \cdot t\right) - \ln\left(-Q\right) \right), \quad (2.16)$$

with restrictions

$$I \in [0; I_{max}]; \; t \in [0; t_{max}]. \quad (2.17)$$

Coefficients models of mathematical type were determined using the method of least squares on the basis of experimental data for lithium-ion type 2170 battery. When checking the adequacy of the mathematical model of the discharge characteristic of the lithium-ion battery type 2170, it was established that with a confidence probability of 0.99 the mathematical model is adequate throughout the discharge characteristic, Figure 2.10.

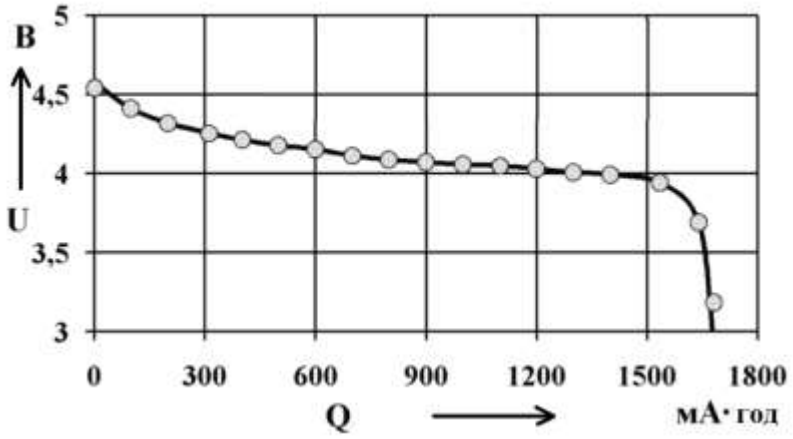

Figure 2.10 – Calculated and experimental characteristics for discharge of a type 2170 lithium-ion battery.

The replacement scheme choice of the, which is described using, as rule, fundamental laws of the theory of electric circuits, is justified by simplifications in the description mathematical between the battery discharge voltage relationship and the duration of the discharge.

When constructing the mathematical model, were not taken following parameters battery lithium-ion:

- the effect of temperature on the output voltage;
- battery self-discharge;
- battery degradation changes related to the time of use;
- heat release of batteries.

The on-board charger electric car Tesla are under the rear seat cushion located. Main right charger are installed on all cars. Some models may have an additional charger on the left side. Each charger is attached to the floor panel with four studs and nuts.

The standard on-board charger with a capacity of 10 kW is compatible with the input ranges:

- voltage from 85 V to 265 V;
- frequency from Hz to 65 Hz;
- current from 1 A to 40 A.

Efficiency charger peak reaches 92%.

In Figure 2.12 HVIL high-voltage junction box and, as we see, Tesla Model S charger circuit are shown.

Tesla Model S shows mileage information based on charge battery and consumption charge statistics. This calculation does not take into account altitude differences and possible wind. The slower the car moves, the less air resistance and the longer the mileage. The graph (see Figure 2.13) shows the relationship between speed and maximum mileage and consumption energy and speed.

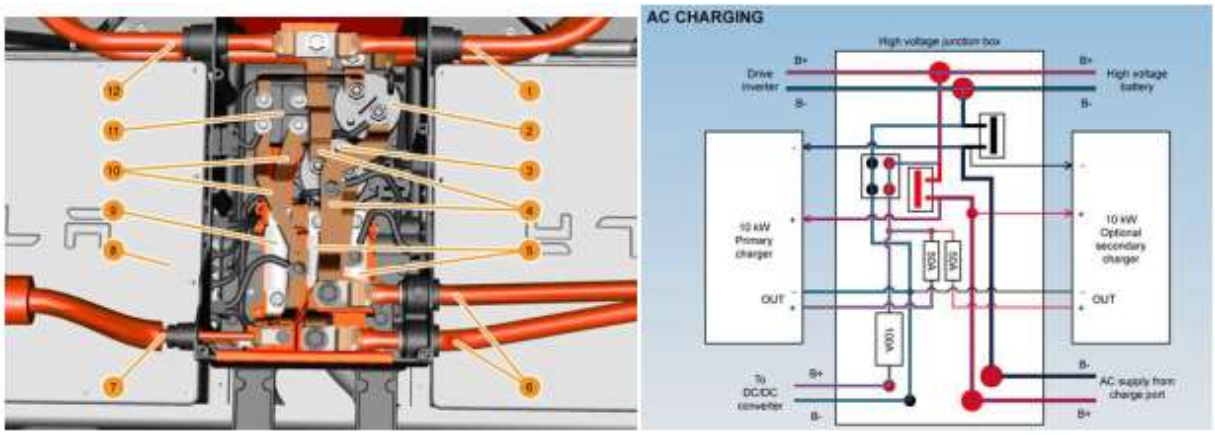

Figure 2.12 – HVIL high-voltage junction box and, as we see, Tesla Model S charger circuit: 1 – high voltage battery; 2 – contact "-"; 3 – "+" contact; 4 – high current buses; 5.9 – fuses 2 for 50 A and 1 for 100 A; 6 – charging port; 7 – direct current input to the converter; 8 – main charger; 10 – low current buses; 11 – noise filter; 12 – drive inverter.

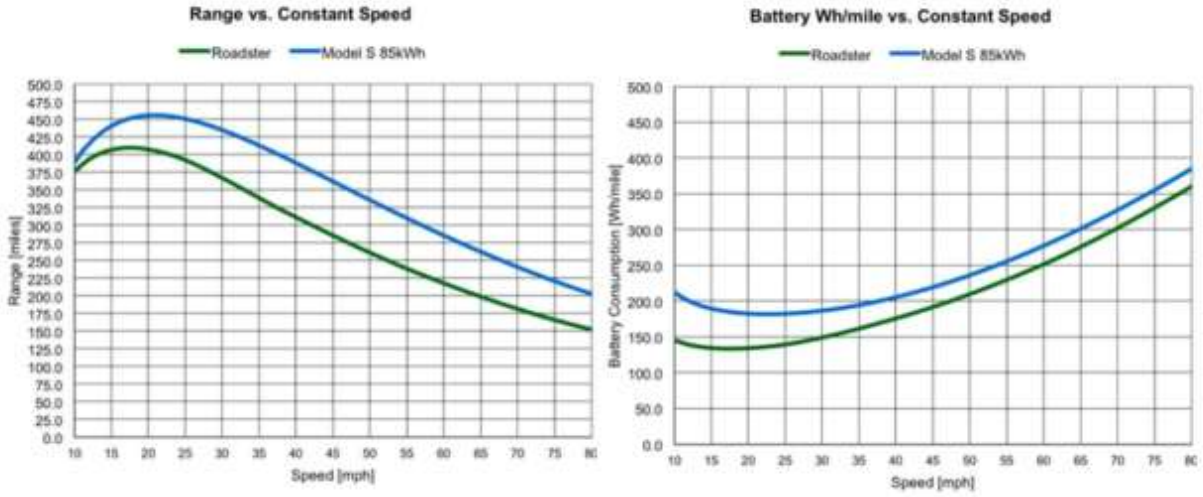

Figure 2.13 – The relationship between speed and maximum mileage, the relationship between speed and consumption energy .

2.3 Active pneumatic suspension.

The active air suspension combines automated benefits with functions that are activated at the request of the driver. The location of the Tesla Model S active air suspension components in Figure 2.14 are shown.

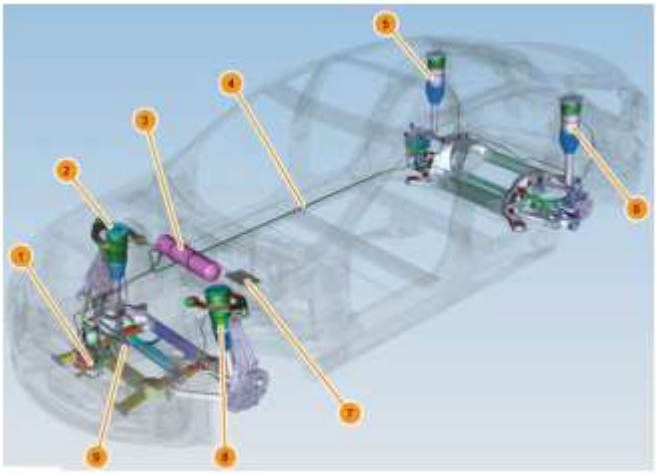

Figure 2.14 – Location of active air suspension components: The components of the front air suspension are shown in Figure 2.15: 1 – air compressor; 2 – RH front suspension module; 3 – tank; 4 – air supply pipes; 5 – RH rear suspension module; 6 - LH rear suspension module; 7 – electronic air suspension control unit (ECU); 8 – LH front suspension module; 9 – block of electromagnetic valves.

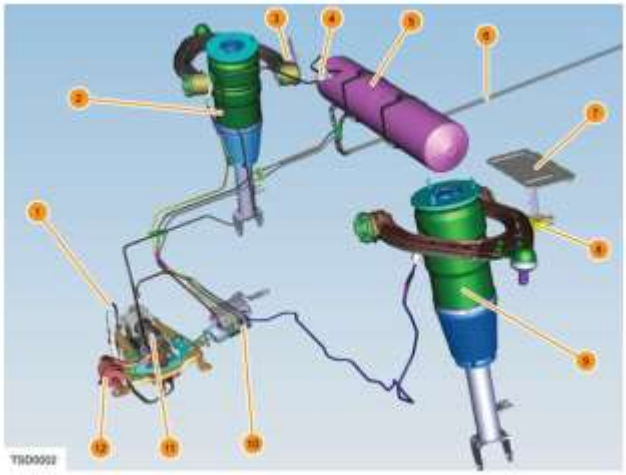

Figure 2.15 - Components of the front air suspension: 1 – ambient air temperature sensor; 2 – RH front suspension module; 3 – RH front height height

sensor; 4 – system filling valve; 5 – tank; 6 – air supply pipes; 7 – electronic air suspension control unit (ECU); 8 – LH front height sensor; 9 – LH front suspension module; 10 – solenoid valve block; 11 – air compressor; 12 - air filter.

The suspension system is powered by air pressure. Air is passed through an air filter to remove any impurities and then drawn into the system by a compressor (see Figure 2.16). The driver can select four levels of active air suspension height using the touch screen: very high; high; standard; low, Figure 2.16.

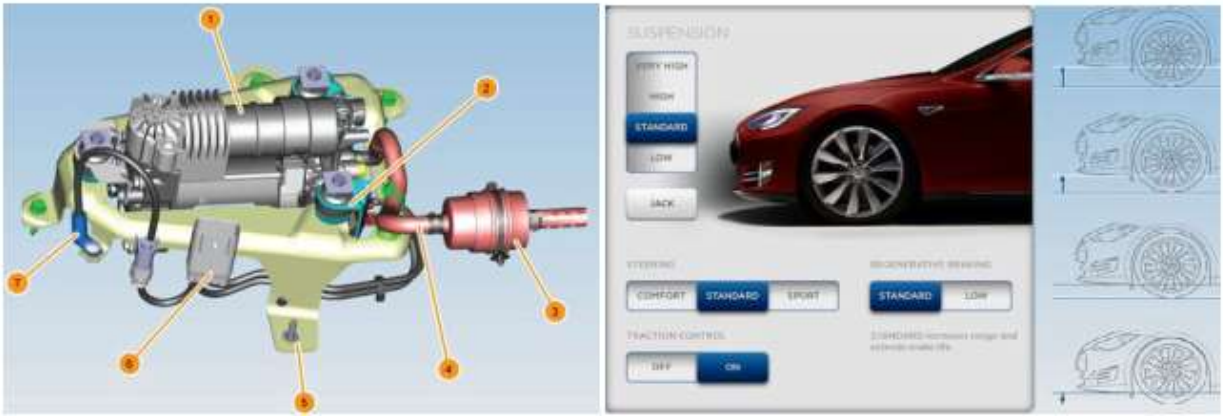

Figure 2.16 - Compressor components and suspension height levels: 1 – air compressor; 2 – rubber assembly; 3 – air filter; 4 - suction hose; 5 – mounting bracket; 6 – electrical connector; 7 - ambient air temperature sensor

2.4 Electronic control stability system.

The ESC system combines in one module all active safety features that help with braking, acceleration and cornering. The following functions are

Present in ESC:

- traction control system (TCS);
- brake assist system (BAS);
- ABS;
- electronic stability control;
- electronic brake force distribution.

Components main of the ESC system in Figure 2.17 are shown.

2.1 Electric power steering.

Electric power steering (EPS) includes a wheel steering, a collapsible steering assembly column, which is to the beam attached of the car, an intermediate shaft consisting lower and upper links, and a steering with an electric drive gear. To the steering mechanism column is connected through an intermediate shaft. Electric power steering and the structural diagram of the EPS unit in Figure 2.18 are shown.

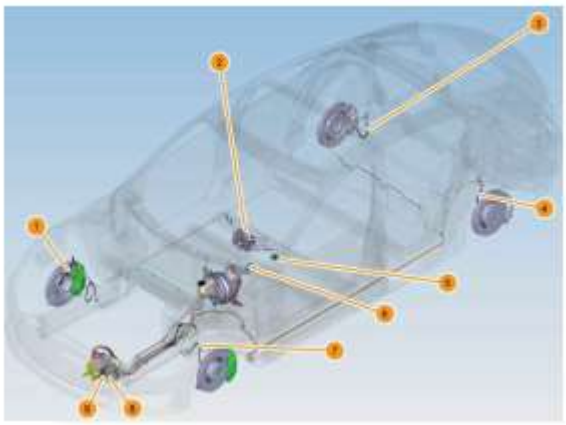

Figure 2.17 – Main components of ESC: 1 - RH front wheel speed sensor; 2 – control angle sensor (SAS); 3 – RH rear wheel speed sensor(WSS); 4 – LH rear VSS; 5 – a set of tilt VSS; 6 – brake pedal; 7 - LH front VSS; 8 – unit control hydraulic; 9 – unit control electronic.

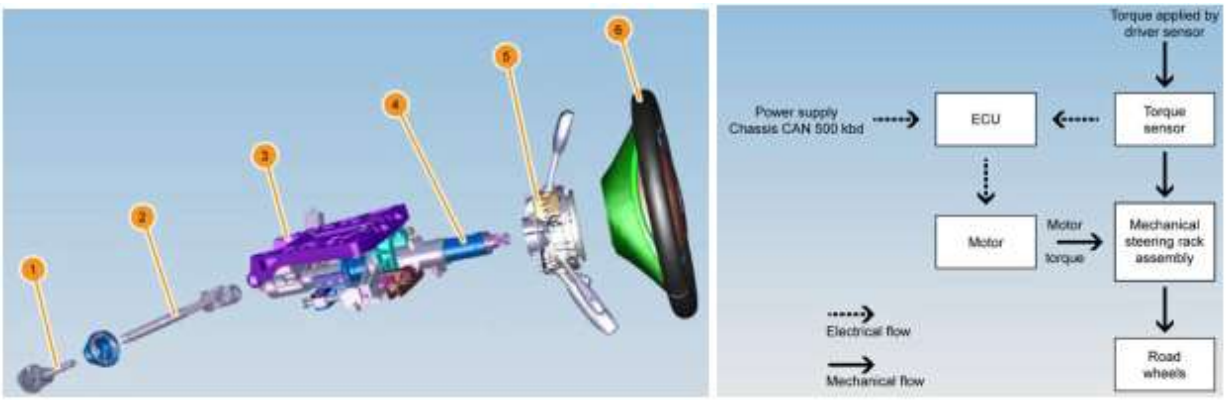

Figure 2.18 – Electric power steering and structural diagram of the EPS unit: 1 – steering wheel; 2 – steering column assembly; 3 – steering rack assembly

2.2 Electromechanical systems of AUDI E-TRONE

We will conduct a study of the electromechanical systems of the AUDI E-TRONE electric car, which, first of all, relate to the subject of the study, namely safety systems.

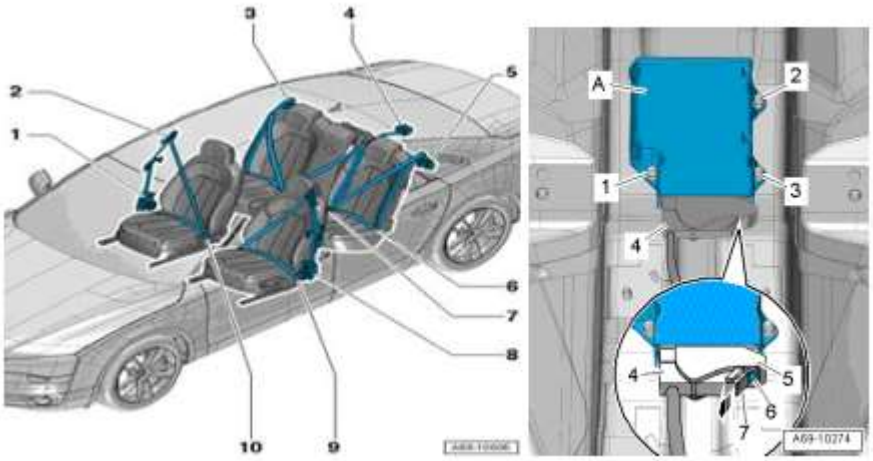

Figure 2.19 – SRS and passive safety system components unit AUDI E-TRONE: 1 - automatic belt retracting mechanism; 2 - seat belt height adjustment mechanism; 3 - mechanism for automatically retracting the seat belt; 4 - mechanism for automatically retracting the seat belt; 5 - mechanism for automatically retracting the seat belt; 6 - fittings for the rear assembly of the seat belt; 7 - rear seat belt lock; 8 - mechanism for automatic retracting of seat belts

with pyro cartridge 1 of the front passenger's belt pre-tensioner, the control unit of the front left seat belt pre-tensioner and the driver's seat belt tension limiter; 9 - accessories of the front seat belt fastening unit; 10 – front seat belt lock.

AUDI E-TRONE seat belts. Seat belts are the main aspect of the protection of the carman and passengers in the event of an accident, as well as to ensure that the driver and passengers are protected during the trip by adjusting the tension of the seat belt by tightening it with an electric motor. The degree of belt tension is adjusted based on many aspects collected by the control unit safety system - SRS. Figure 2.19 shows the seat belt system and the AUDI E-TRONE electric vehicle and passive safety control unit.

2.3 AUDI E-TRONE airbags

The components of airbags are shown in Figure 2.20.

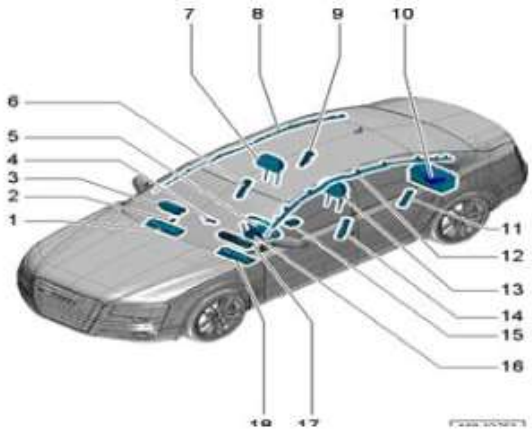

Figure 2.20 - AUDI E-TRONE airbag components and PSC unit:

The numbers at this figure are next: 1 - knee airbag with driver's knee airbag pyro cartridge; 2 - a switch with a lock for turning off the front passenger's airbag; 3 - the front passenger's airbag with the pyro cartridge of 1 airbag and the pyro cartridge of the release valve of the front passenger's airbag; 4 - the control lamp of the front passenger's airbag is off; - the driver's airbag with the pyro cartridge of the driver's airbag and the pyro cartridge of the release valve of the driver's airbag; 6 - side airbag of the front passenger with a pyro cartridge of the side airbag of the front passenger; 7 - active headrest on the side of the front passenger with a pyro cartridge for the active headrest of the front passenger seat 8 - front passenger head protection pillow with pyro cartridge of the front passenger head protection pillow; 9 - rear side airbag on the side of the front passenger with a pyro cartridge of the rear side airbag on the side of the front passenger; 10 - pyro cartridge for unlocking the battery; 11 - rear side airbag on the driver's side with a pyro cartridge of the rear side airbag on the driver's side; 12 - driver's head protection pillow with driver's head protection pillow pyro cartridge; 13 - active headrest on the driver's side with a pyro cartridge for the active headrest of the driver's seat; 14 - the driver's side airbag with the pyro cartridge of the driver's side airbag; 15 - airbag control unit; 16 - steering column electronics control unit with a flat spring-shaped conductive element for an airbag and a contact ring and a steering wheel rotation angle sensor; 17 - airbag control lamp; 18 - driver's knee airbag with driver's knee airbag pyro cartridge.

2.4 AUDI E-TRONE shock sensor.

Impact sensors and their location in an electric vehicle are shown in Figure 2.21.

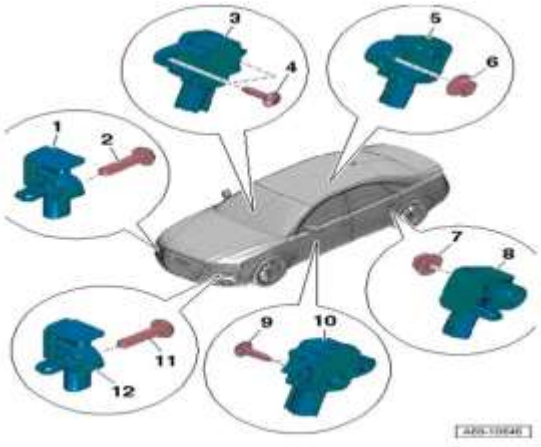

Figure 2.21 - Impact sensors and their location: 1 - impact sensor of the front passenger's front cushion; 3 - impact sensor of the side airbag of the front passenger; 5 - impact sensor of the rear side airbag of the front passenger; 8 - impact sensor of the rear side airbag on the driver's side; 10 - impact sensor of the side airbag on the driver's side; 12 - impact sensor of the driver's front cushion.

3 DEVELOPMENT OF AN ELECTRIC VEHICLE SAFETY SYSTEM AGAINST A SIDE COLLISION

When developing a safety system for an electric vehicle against a side collision, it is necessary to conduct a study of the system, which should record the safety of a side collision. Such systems have the properties of machine vision and can be built according to different operating principles.

3.1 Principles of building a machine vision security system

Machine vision enables the safety system of an electric car (with the help of technical means of measurement and further computer mathematical processing) to remotely sense and receive information about the environment for further analytical processing.

We will analyze approaches to building machine vision systems. The conducted research allows us to classify four different technical approaches to the design of technical vision devices for autonomous cars:

- methods based on the use of a video camera;
- methods based on the use of laser scanning systems;
- methods based on GPS navigation;
- methods based on the use of ranging (radiolocation, sonar, laser principles, etc.).

For the machine vision of the safety system of an electric vehicle, it is based on the detection of the fact of movement (or quasi-static movements) within the field of vision. Let's consider each of these methods in more detail.

3.2 Machine vision based on the use of video cameras.

The machine vision system includes two (or four) television cameras mounted together and data processing equipment. The system detects obstacles in real time within its field of vision in the range from 5 m to 50 m in front of the vehicle with a viewing angle of 40 degrees. The cameras are located vertically in the front part of the vehicle. The system finds obstacles in the trapezoidal field of view. When scanning, the cameras are synchronized, and in order to implement a high speed of processing video signals from the cameras, the processing unit uses circuit-implemented logic instead of programmable devices. The principle of obstacle detection is based on parallax. When two images from both cameras are compared, the two images of the obstacle are identical except for the position in the coordinate system tied to the machine vision system. On the other hand, each image of an element on the ground is different due to the position of the cameras. Figure 3.1 illustrates the principle of obstacle detection.

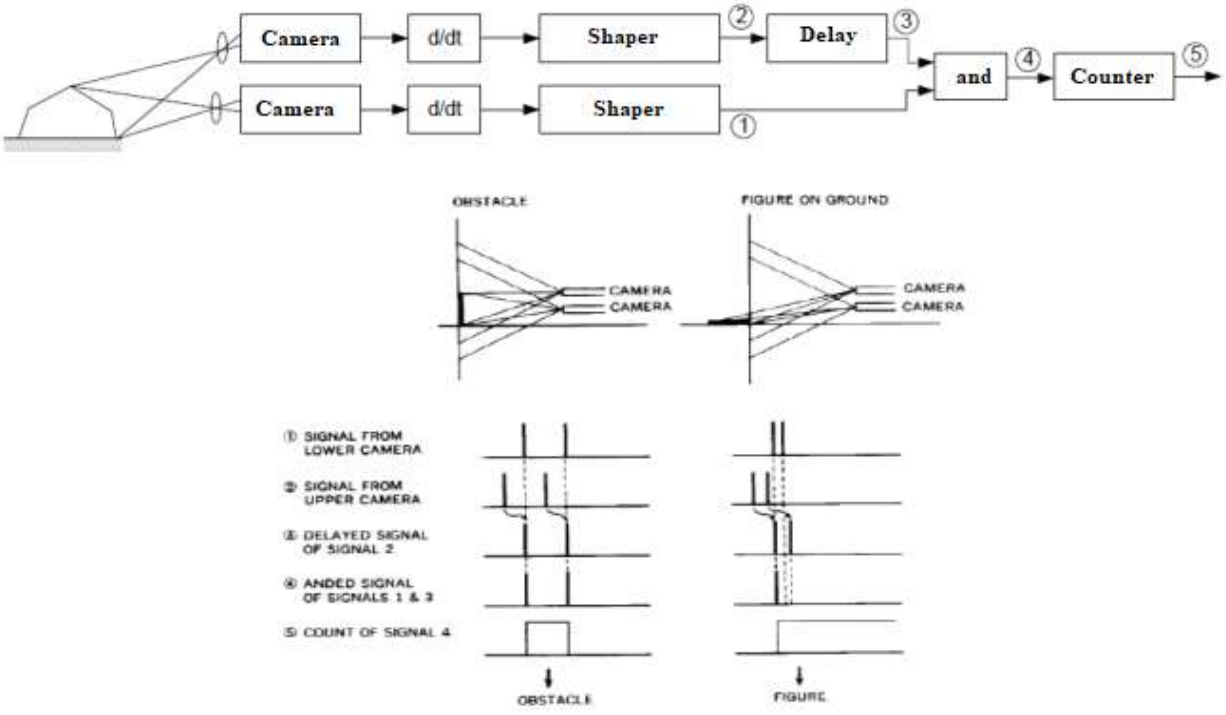

Figure 3.1 – The principle of detecting obstacles in real time

Video signals are differentiated by time and pulses are formed that correspond to the edges of the images. Each time interval of pulses from each camera (signal 1 and signal 2 in Figure 3.1) distinguishes the obstacle from the element on 40 road.

An obstacle generates the same time slots, while an element on the road generates different time slots. The cameras must therefore be synchronized with each other, and must use vertical and progressive scanning methods. The position of the sweep line corresponds to the direction of the obstacle, and the point where the optical axes of the cameras intersect indicates the distance to the obstacle. The delay of one of the signals from the cameras is equivalent to the rotation of the optical axis of the camera. Thus, changes in time delays allow us to detect interference in other locations.

To expand the field of view and detect an obstacle in the two-dimensional field of view during one scanning period, parallel processing of 16 types of delay is carried out, which gives a field of view of 16 zones located longitudinally at an interval of 1 m. The time required to detect obstacles is 35.6 ms, which consists of 33.3 ms of scanning one frame and 2.3 ms of processing to detect the position of the obstacle.

The basis of any method using a camera is the principle of three-dimensional human vision, capable of reconstructing a three-dimensional image and approximately estimating the distances to objects in the field of view, that is, in other words, stereoscopic vision.

Any technical system of stereoscopic vision is a multi-camera system. In this simple case, these are systems with two cameras. If a stereoscopic vision system is used and the 3-D point is visible on both the left and right images (see Figure 3.2), then s can be used as visual characteristics (the vector s contains the required values of the field of view / characteristics) [8]

$$s = xs = (xl, xr) = (xl, yl, xr, yr), \tag{3.1}$$

that is, to represent the point only by convolution in s of the x and y coordinates of the observed point in the left and right images.

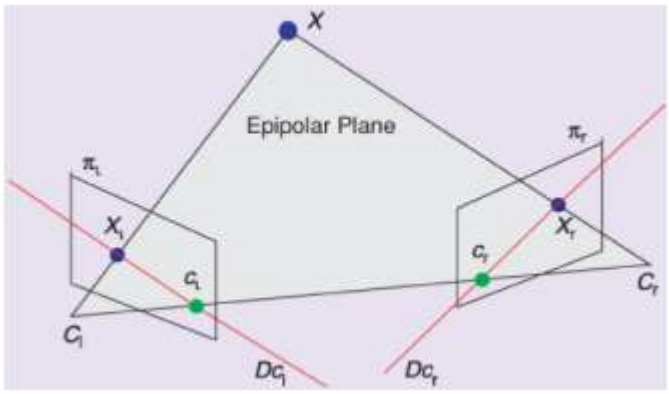

Figure 3.2 – Stereo vision system

For a 3-D point with coordinates X = (X,Y,Z) in the camera frame, which are projected in two images as a two-dimensional point with coordinates x = (x,y), we have [19]

$$\begin{cases} x = \dfrac{X}{Z} = \dfrac{u - c_u}{f \cdot \alpha} \\ y = \dfrac{Y}{Z} = \dfrac{v - c_v}{f \cdot \alpha} \end{cases}. \tag{3.2}$$

The matrix of image dimensions m=(u,v) gives the coordinates of the image point, expressed in pixels, and a = (cu, cv, f,) is a set of the camera's own parameters: cu and cv are the coordinates of the main point, f is the focal length, and - image pixel aspect ratio. In this case, we take s=x=(x,y) - coordinates of the image of the point on the plane. Taking the time derivative from the projection of equations (1.2), we will obtain a result that can be written in general form:

$$X = Lx\ Vc(vc, \omega c), \tag{3.3}$$

where Lx – matrix of interconnection;

$Vc(vc, \omega c)$ is the spatial velocity of the camera Vc., which depends on vc, ωc;

vc is the instantaneous linear velocity of the coordinates of the frame of the camera frame;

ωc is the instantaneous angular speed of rotation of the camera frame;

Suppose that the matrix of interconnection Lx controls the movement of the camera with six degrees of freedom, which are related to the vector x as follows

$$Lx = \begin{bmatrix} -\frac{1}{z} & 0 & \frac{x}{z} & xy & -(1+x)^2 & y \\ 0 & -\frac{1}{z} & \frac{y}{z} & 1+y^2 & -xy & -x \end{bmatrix}. \quad (3.4)$$

In the matrix Lx, the z value is the depth of the point in relation to the frame of the camera frame. Thus, any control system that uses this form of matrix relationship must estimate or approximate the value of z. Similarly, the camera's own (internal) parameters are involved in the calculation of x and y.

Let's analyze these main parameters of the "camera-based method" based on equations (3.2) - (3.4):

- the focal length f in (3.2), as well as a set of internal parameters of the camera, shows us that the error of the camera is closely related to manufacturing imperfections of each specific camera. Therefore, the absolute value of the error of this camera increases significantly with an increase in the scanning depth (in proportion to 1f, 2f ... nf);

- Vc in formula (3.3), ie the speed of the camera, shows us that any methodological error of the camera is closely related to the camera's own motion. And, given the random nature of the camera's own motion, and, therefore, the

instantaneous directions of the Vc vector, it is very difficult to estimate the real error of the camera;

- the depth z in (3.4) shows that the methodological resolution and acceptable speed are limited by the own theory of this method.

These reasons allow us to understand quite clearly the fundamental limitations for any practical application of camera-based technical vision methods. They are very important for practical use in any applications with positioning of the camera's own movement, make cameras extremely sensitive to any vibrations and dynamic actions. Moreover, despite the significant advances in camera-based technology over the last ten years, there is still the possibility of "camera error," that is, when the image of one typical object is associated with the typical properties of another. And this opportunity increases in proportion to the increase in distance. Finally, practical applications using camera-based methods are limited to a distance of up to 50 m.

3.3 Machine vision based on the use of lasers.

Modern technologies of laser sensors have made it possible to collect fast and accurate 3-D data, as evidenced by several commercial 3-D laser installations [21, 22]. In addition, some existing 3-D technologies are based on a charge-coupled device (CCD) with two-dimensional image reconstruction. These 3-D sensors are based on laser scanning and geometric methods, such as triangulation [23,24], and have been widely developed in machine vision applications due to their reliability and simplicity. However, in order to expand the functional applications of these laser sensors, powerful built-in additional algorithms are still needed for efficient processing of the data measured by them, depending, as a rule, on specific cases of application.

The principle of laser triangulation in general can be based on two schemes, presented in Figure 3.3, a, b. The first principle uses a fixed radiation angle and a

variable distance, and the second, on the contrary, a constant triangulation base and a variable scanning angle.

The principle of laser triangulation with a fixed radiation angle works as follows. The laser beam is projected onto the measured surface (see Figure 3.3, a), where it is diffusely reflected from the surface and its image is determined by the optical receiver. With the help of the agreed angular location between the laser and the sensor, the detection of the position of the laser spot on the image plane allows for accurate measurement of the distance between the sensor and the surface.

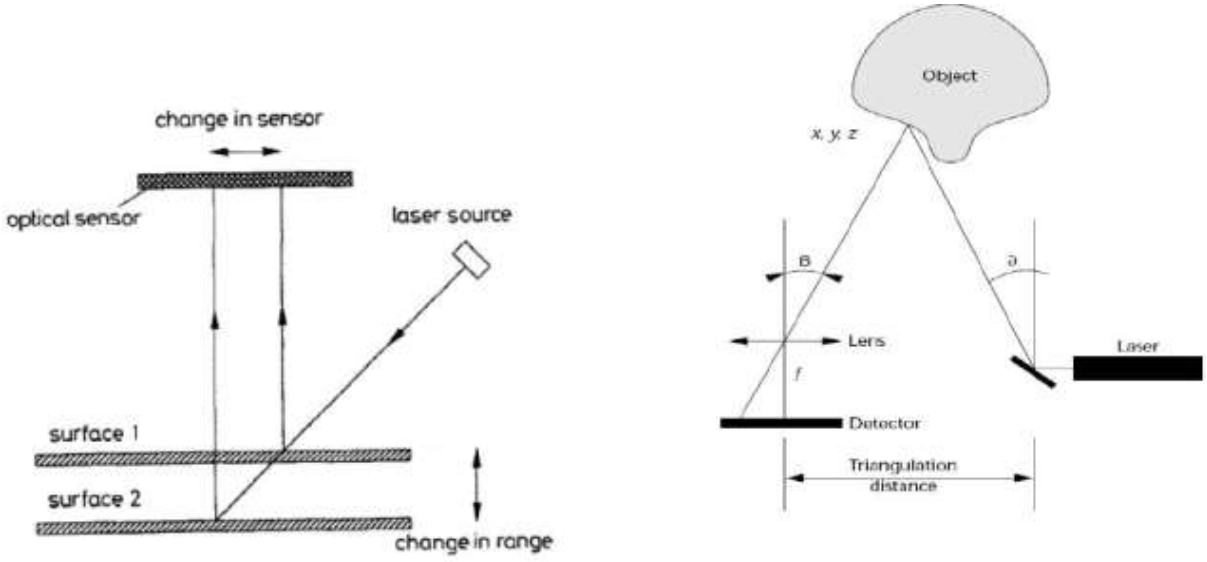

a) b)

Figure 3.3 – Two principles of laser triangulation: a – with a fixed radiation angle, b – with a fixed basic triangulation distance.

The laser beam scans the entire visible surface of the object. The series of data from each position is calculated according to its position on the plane, so that the entire three-dimensional profile of the surface can be obtained step by step. The position of the laser beam is usually controlled by an adjustable mirror system that can change the angular position of the laser beam on the plane.

The second basic triangulation scheme (see Figure 3.3, b) is an active optical triangulation 3D discretizing system that visualizes real objects. These active optical systems provide photorealistic representation of shapes and textures at an

acceptable speed. Figure 3.3, b shows the scheme of the triangulation scanner. The laser beam reflected from the mirror is projected onto the object. Diffuse reflected light is collected by a sensor. The sensor forms a linear array (vector) if a laser point is projected, and a two-dimensional matrix if a laser stripe is projected. The angle δ is controlled (see Figure 3.3, b) by the laser positioning scheme and is considered known. The angle β is determined by measuring with a sensor, if the focal length f and the pixel size of the receiver are given. Triangulation and the distance between the sensor and the mirror is also known.

As can be seen from Figure 3.3, b, the coordinates x, y, z of a point on the object can be calculated by trigonometric methods since all geometric parameters are known. If one laser point is projected, the system measures the coordinates of only one point of the object. When a laser beam is projected, all points along the beam are digitized. The triangulation scheme can be improved to improve optical quality and depth of field. The changes, however, require custom-made components and are relevant mainly for scanners used in high-precision reengineering tasks. In general, any other type of structured light can replace a point or strip laser. For example, multiple points or laser lines can be projected.

However, if the system projects several images, it is difficult to identify individual elements. If, say, two bands are projected, the imaging software must separate the first and second bands. Solutions to the identification problem include the use of different sequences of colored bands. Such circuits usually become sensitive to illumination, which we will discuss later. The most famous optical triangulation 3D scanner was developed by the Cyberware company from Monterey, California (USA).

Cyberware products can capture photorealistic images of a range of objects – from models the size of an apple to the full-size human body. The scanner head contains a laser radiation generator, a system of mirrors, and black-and-white and color video cameras. Scanning is carried out by moving the object on a rotating or moving platform, or by moving the sensor around the object in a circular motion.

In the basic model of the Cyberware scanner, a system of mirrors collects laser light from the left and right triangulation directions in relation to laser.

This scheme allows you to avoid shadows during scanning caused by the angle of triangulation. However, this design imposes strict requirements on the quality of optics assembly and system calibration, and also increases the size of the scanner. Scanners are complex, non-portable, and prohibitively expensive for many applications. In the most advanced version, scanners digitize the entire human body as a combination of four scan images in about 17 seconds. Each scan has a resolution of 250 × 1000 points. The four scans can be combined using commercial software packages.

Another typical method for laser scanners is a circular laser scanning vision sensor that determines the position of special (singular) points. This is usually the name of a scanning sensor for collecting data with a circular scanning area and with a rotating head (CSS). In this case, by a singular point we mean a small convex or concave point deviation from various smooth surfaces, caused either by a malfunction or by a normal manufacturing/machining defect. The platform for this device has three degrees of freedom for motion control using a processor, three servo motors and a circular scanning sensor (CSS), as well as a computing system. The radiating head is hard-wired with CSS to display tracking and focusing actions, Figure 3.4.

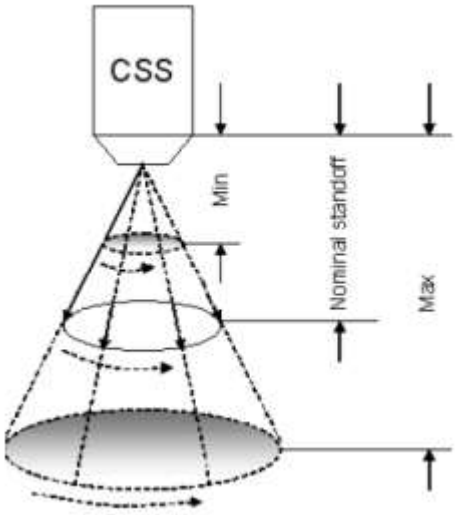

Figure 3.4 – Illustration of the principle of circular scanning

A circular scanning sensor (see Figure 3.4), with a built-in data acquisition device, is a laser scanning multi-axis machine vision device that receives a sequence of 3-D data about a part of the surface of the object under study to reconstruct its geometric characteristics.

The engines are controlled by the central processor, which receives information about the position of singular points from the computer system. The loop is then closed by returning the 3D geometric data about the target object points obtained by CSS to the computer system, which processes the continuously obtained data using algorithms to recover information about the position of singular points, if any, on the part of the surface under study . The order of data processing is shown in Figure 3.5.

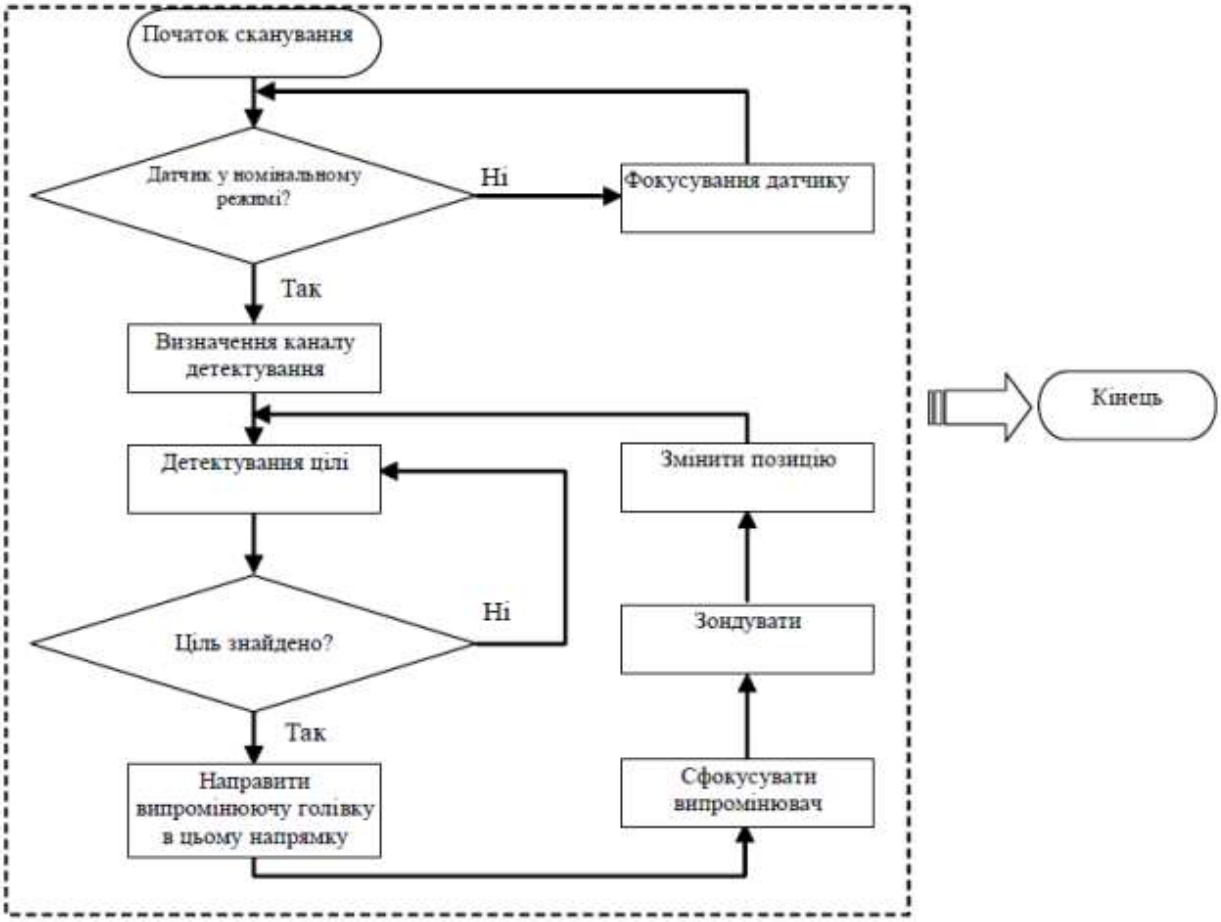

Figure 3.5 – Data processing procedure

Scanning Sensor for Data Collection with Circular Scanning Area The radiating head is controlled by three servomotors to create 3-D (x, y, z) motion: horizontal, near-planar, up and down motion. The driver of the main emitting head can track any three-dimensional singular points on the surface of the working area while scanning and collects them at the specified focal distance. For the central laser scanning sensor, a sequence of scanning data is obtained

$$Xi = [x0, x2, \cdots, xN-1], i = 1, 2, \cdots N-1, \quad (3.5)$$

where Xi is the sequence of data captured in the i-th interval; N is the number of scanning time intervals, which is called the depth of the data sequence. The sequence of data Xi can represent part of the data received by one sensor at different predetermined time intervals, or by several sensors at the same time. For example, a linear or circular scanning laser sensor generates a geometric sequence their data about the object in one scan cycle. If we consider the data from the circular sensor, then the depth N is also the period of the scanning cycle.

Machine vision based on the use of GPS and combined systems.

GPS-based solutions are also sometimes acceptable for machine vision, especially for navigation tasks. GPS navigation for autonomous ground vehicles has GPS capabilities for determining the location of vehicles as well as static objects based on signals from satellites [22, 23].

GPS measurement systems consist of biased and noisy estimates of ranges of distances to orbiting satellites.

The main source bias is the unknown offset of the receiver's clock, and other errors arise as a result of:

- modulation of the satellite clock and ephemeris;
- modulation of ionospheric and tropospheric delays;
- the influence on the result of the measurement of the code and phase of both the noise of the receiver and the type of interference that carries the multivariate path of the probing signal (multipath).

DGPS technology improves the accuracy of determining the user's location by measuring infinitesimally small changes in variables in order to provide corrections to the satellite's positioning. It must have a base station, a data channel, and user applications. The base station generates corrections by measuring the pseudo distance and carrier frequency range, and calculates the distance from the base station to each satellite and the satellite clock offset, and estimates the receiver clock offset, and communicates this information to the user application. The correction messages contain the Pseudo Range Correction PRC for DGPS, the Carrier Phase Correction CPC for CDGPS and their changes in time t, the Range Rate Correction RRC

$$PRC=-(-b+I+T+\delta R)=d-\rho+\bar{B}\,, \tag{3.6}$$

$$CPC=-(-b+I+T+N\lambda)=d-\varphi+\bar{B}\,, \tag{3.7}$$

where ρ - the pseudo-distance measurement;

φ – carrier frequency phase measurement;

λ - the wavelength of the carrier frequency;

N – integer uncertainty;

d - the distance from the base station to the satellite;

b – satellite clock offset error;

B – estimate of the offset of the receiver clock;

I – ionospheric delays;

T – tropospheric delay;

δR - the orbit error (orbital error). Unfortunately, the available accuracy for civil applications is not high, given the large inaccuracy of all the main terms in formulas (3.6, 3.7). Above all, objective atmospheric delays (ionospheric and tropospheric). Although the accuracy of commercial DGPS (Differential GPS) increases to several meters, it is therefore possible to use image processing tools to compensate for this error. Despite the fact that it is difficult to use image

processing to recognize a complex environment, its use is possible to identify and recognize some specific objects that have a simple appearance.

3.4 Construction of the safety system of an electric vehicle against a side collision

Side collision safety systems of an electric vehicle must work in conjunction with other passive and active safety systems of an electric vehicle. Therefore, we will conduct an analysis and study of the electrical connection of security systems. The passive safety management system of an electric vehicle includes such elements as:

- safety system control unit;
- safety belts;
- high-voltage fuse;
- low-voltage fuse;
- inflatable curtains;
- knee airbags;
- seat belt pre-tensioner;
- shock sensors;
- airbags for the driver and front passenger.

Analyzing data from impact sensors located in front and behind the car, as well as in the doors, the control unit calculates exactly when and with what effort to activate the airbags and seat belts. Figure 3.6 - 3.8 shows electrical diagrams and all components of the passive safety system using the Tesla Model X electric car as an example.

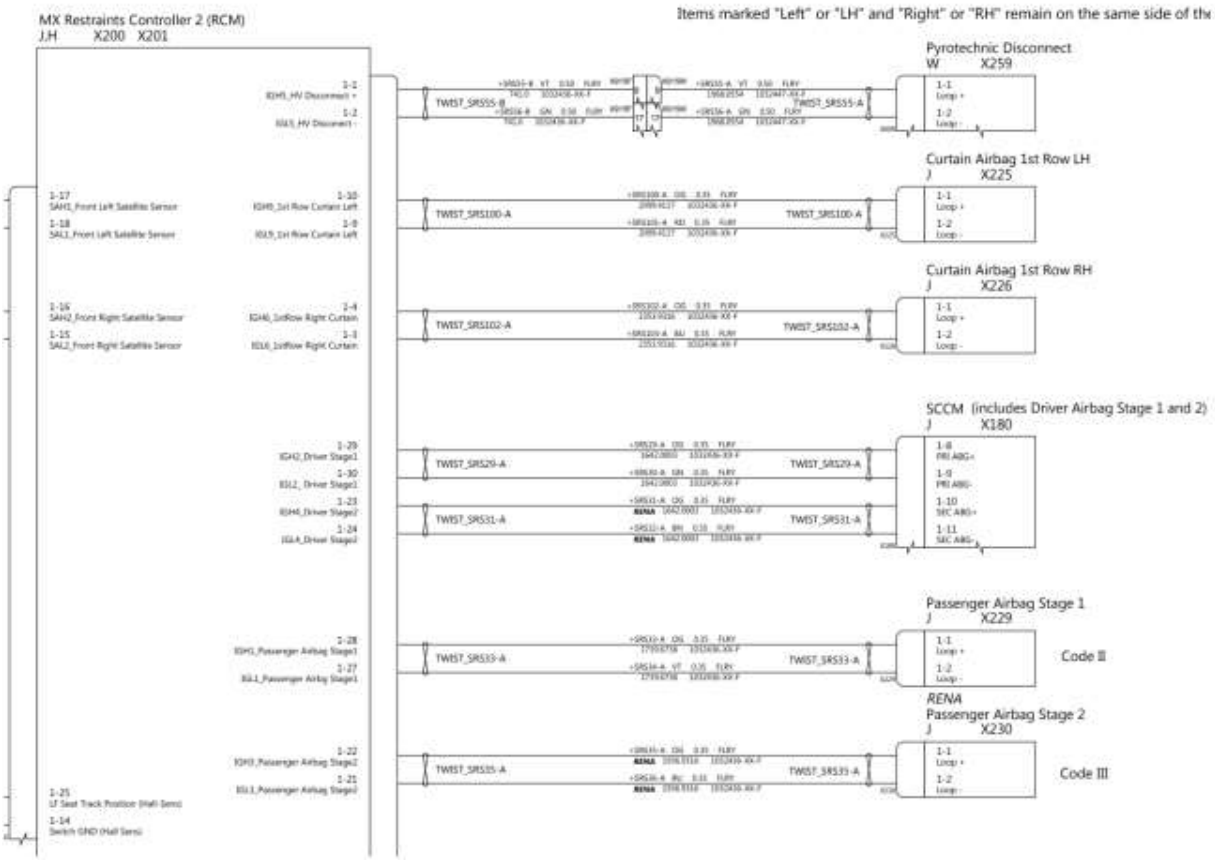

Figure 3.6 – Electrical scheme 1 of the passive safety system of the Tesla Model X electric car: - X202 Impact sensor front left; 2 - X203 Impact sensor front right; 3 - X940 Front passenger seat position sensor; 4 - X259 High-voltage fuse; 5 - X225 Inflatable curtain left; 6 - X226 Inflatable curtain right; 7 - X180 Driver's airbag; 8 - X229, X230 Front passenger airbag; 9 - X231 Pyro-cartridge for inflating the passenger airbag; 10 - X232 Driver's knee airbag; 11 - X233 Knee airbag of the front passenger; 12 - X200, X201 SRS system control unit;

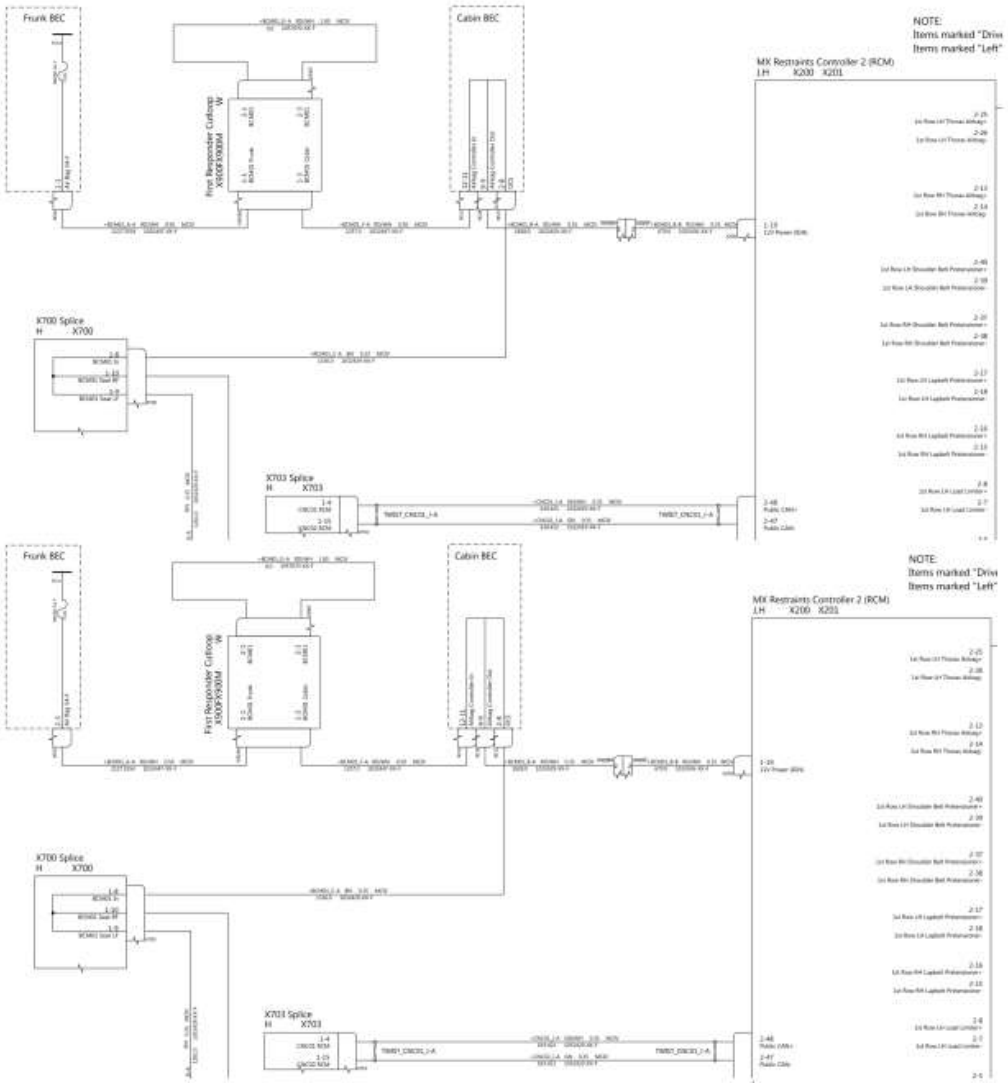

Figure 3.7 – Diagram of electrical circuit 2 of the passive safety system of the Tesla Model X electric car: 1 - X900 Service connector for connecting a high-voltage battery; 2 - X940 Position sensor of the second row of left seats; 3 - X945 Position sensor of the second row of seats, right; 4 - X200, X201 SRS system control unit; 5 - X237 Left front seat airbag; 6 - X238 Right front seat airbag; 7 - X217 Seat belt pretensioner of the upper left front seat; 8 - X218 Front seat belt pretensioner, upper right; 9 - X215 Lower left front seat belt pretensioner; 10 - X216 Lower left front seat belt pretensioner; 11 - X221 Front load limiter seat of the left; 12 - X222 Load limiter of the right front seat; 13 – X241 Left curtain; 14 – X242 Right curtain; 15 - X219 Retractor of the second row of the left seat; 16 - X220 Retractor of the second row of the right seat; 17 - X235 Airbag of the second row of the left seat; 18 - X236 Airbag of the second row of the right seat;

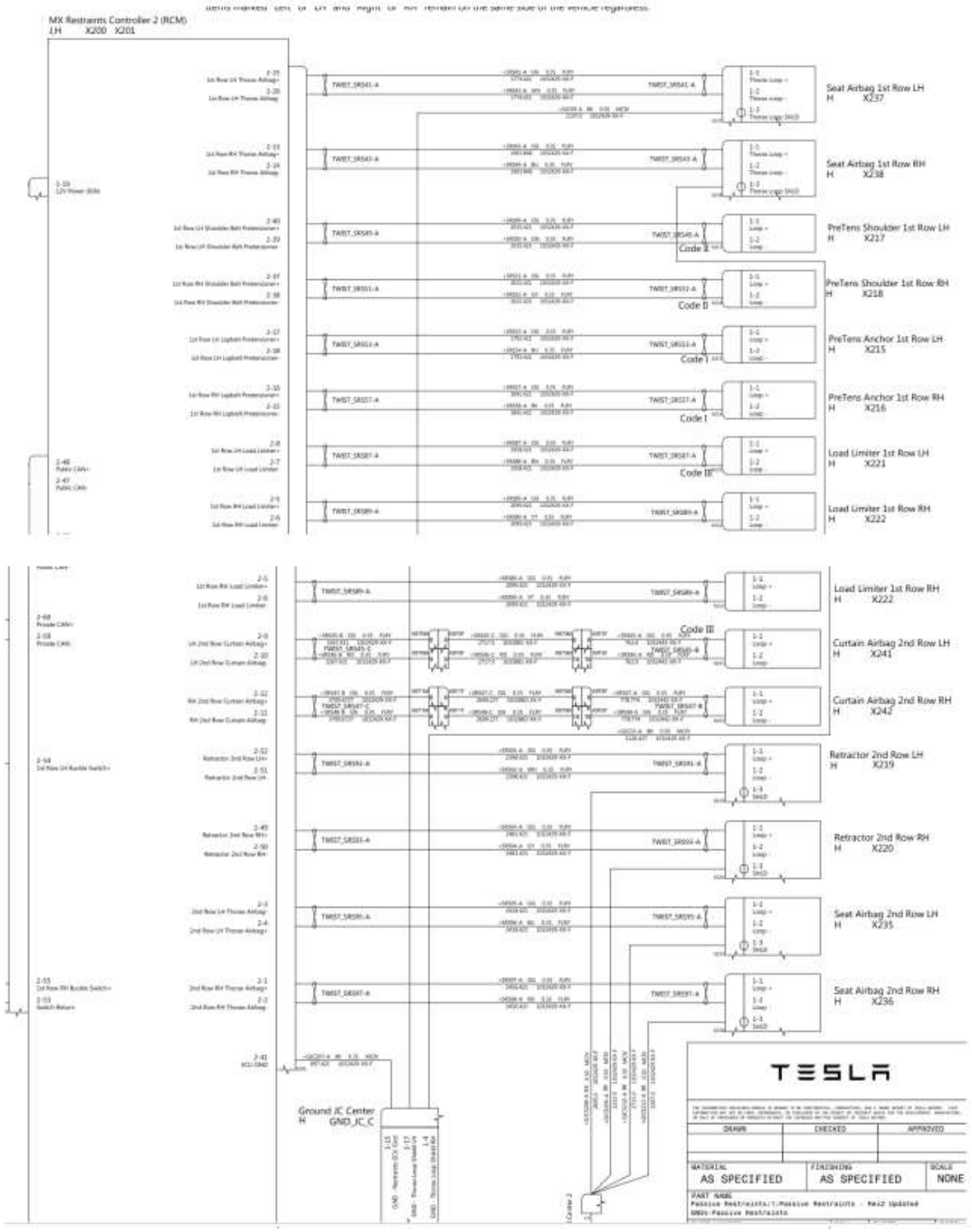

Figure 3.8 – Electrical diagram 3 of the passive safety system of the Tesla Model X electric car: 1 - X204 Side impact sensor of the front left door; 2 - X205 Side impact sensor of the front right door; 3 - X207 Impact sensor front left; 4 - X206 Impact sensor front right; 5 - X208 Impact sensor rear left; 6 - X209 Impact sensor rear right; 7 - X213 Impact sensor central rear;

An example of the operation of the AUDI side collision safety system is shown in Figure 3.9.

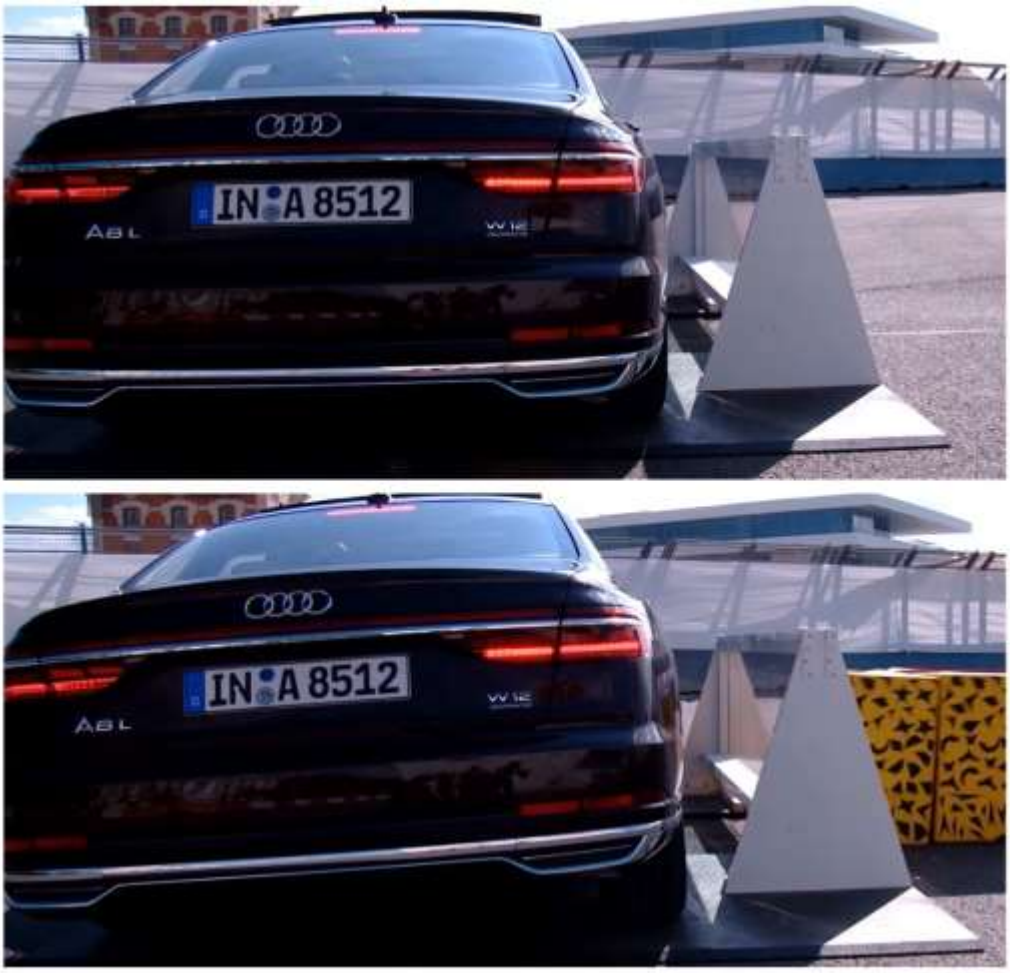

Figure 3.9 – Example of operation of the AUDI side collision safety system

Sensors in the height adjustment system are used to adjust the height of the suspension on the road and in emergency cases to prevent accidents. The location of the body position sensors for the side impact protection system and the AUDI electro-pneumatic suspension is shown in Figure 3.10. The communication network of the components of the side impact protection system and the AUDI electro-pneumatic suspension is shown in Figure 3.11.

The side impact control system analyzes a large number of parameters, based on which it calculates the moment when the shock absorbers are activated.

Parameters by which this system works: - body position sensors; - front and rear view radar; - parking sensors; - proximity sensors in the side doors; - circular inspection system.

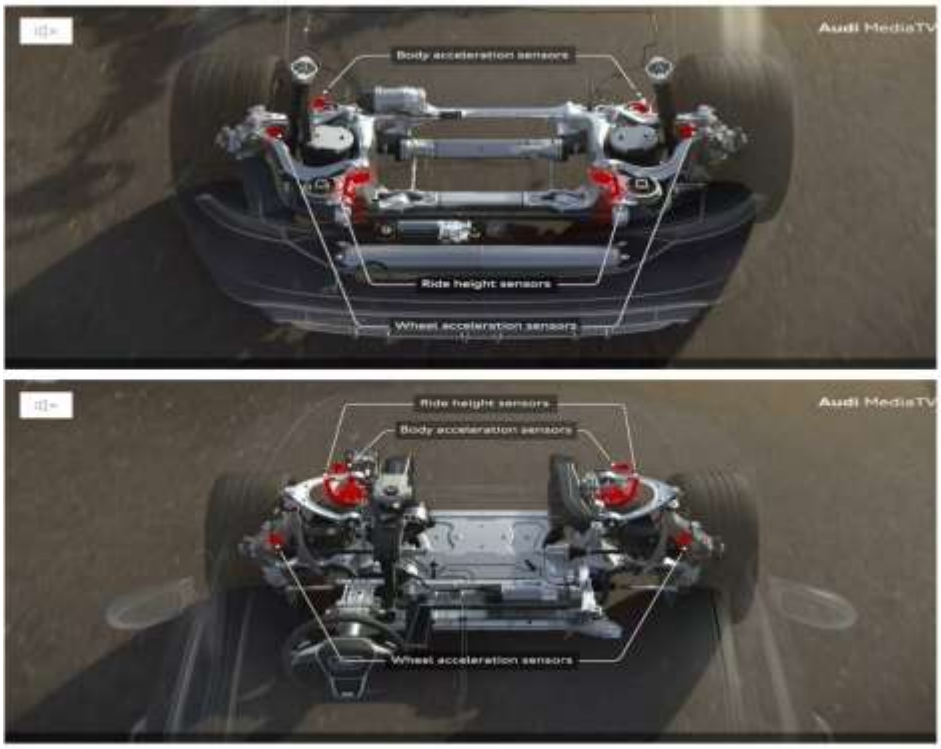

Figure 3.10 – Location of body position sensors for the side impact protection system and the AUDI electropneumatic suspension

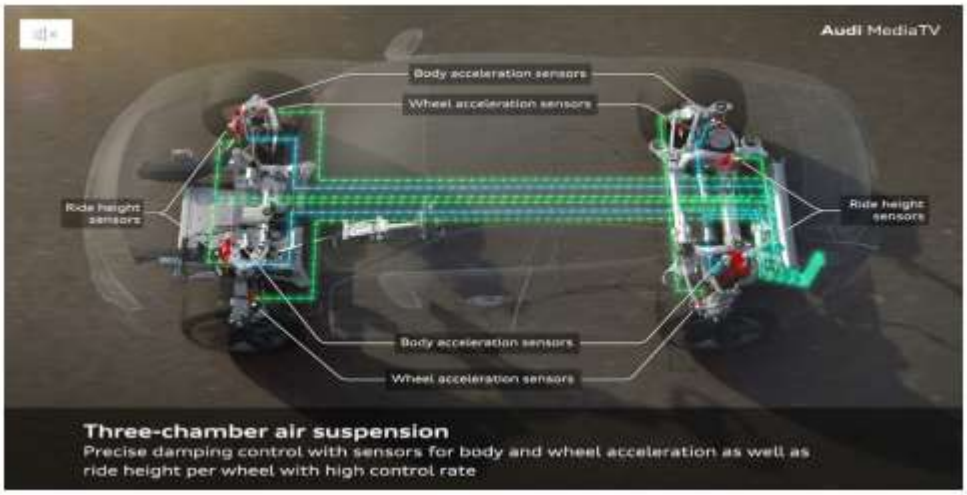

Figure 3.11 – Communication network of the components of the side impact protection system and the AUDI electro-pneumatic suspension

The arrangement of the pneumatic shock absorber rack with variable height of the AUDI car is shown in Figure 3.12.

Figure 3.12 - Arrangement of a pneumatic shock absorber rack with a variable height of the car

The shock absorber (see figure 12) consists of three sections, in which air or nitrogen is located. The first chamber of the shock absorber works during normal driving on flat roads. The second and third cameras work when there is a request to change the height of the suspension.

4 OCCUPATIONAL HEALTH AND EMERGENCY SAFETY

4.1 Effects of electromagnetic radiation on the human body

A large body of literature exists on the response of tissues to electromagnetic fields, primarily in the extremely-low-frequency (ELF) and microwave-frequency ranges. In general, the reported effects of radiofrequency (RF) radiation on tissue and organ systems have been attributed to thermal interactions, although the existence of nonthermal effects at low field intensities is still a subject of active investigation. This chapter summarizes reported RF effects on major physiological systems and provides estimates of the threshold specific absorption rates (SARs) required to produce such effects. Organ and tissue responses to ELF fields and attempts to characterize field thresholds are also summarized. The relevance of these findings to the possible association of health effects with exposure to RF fields from GWEN antennas is assessed**.**

Nervous System

The effects of radiation on nervous tissues have been a subject of active investigation since changes in animal behavior and nerve electrical properties were first reported in the Soviet Union during the 1950s and 1960s.1 RF radiation is reported to affect isolated nerve preparations, the central nervous system, brain chemistry and histology, and the blood-brain barrier.

In studies with in vitro nerve preparations, changes have been observed in the firing rates of Aplysia neurons and in the refractory period of isolated frog

sciatic nerves exposed to 2.45-GHz microwaves at SAR values exceeding 5 W/kg.2,3,4 Those effects were very likely associated with heating of the nerve

preparations, in that much higher SAR values have not been found to produce

changes in the electrical properties of isolated nerves when the temperature was controlled.5, 6 Studies on isolated heart preparations have provided evidence of bradycardia as a result of exposure to RF radiation at nonthermal power densities,7 although some of the reported effects might have been artifacts caused by currents induced in the recording electrodes or by nonphysiological conditions in the bathing medium.8,9,10 Several groups of investigators have reported that nonthermal levels of RF fields can alter Ca2+ binding to the surfaces of nerve cells in isolated brain hemispheres and neuroblastoma cells cultured in vitro (reviewed by the World Health Organization11 and in Chapters 3 and 7 of this report). That phenomenon, however, is observed only when the RF field is amplitude-modulated at extremely low frequencies, the maximum effect occurs at a modulation frequency of 16 Hz. A similar effect has recently been reported in isolated frog hearts.12 The importance of changes in Ca2+ binding on the functional properties of nerve cells has not been established, and there is no clear evidence that the reported effect of low-intensity, amplitude-modulated RF fields poses a substantial health risk.

Results of in vivo studies of both pulsed and continuous-wave (CW) RF fields on brain electrical activity have indicated that transient effects can occur at SAR values exceeding 1 W/kg.13,14 Evidence has been presented that cholinergic activity of brain tissue is influenced by RF fields at SAR values as low as 0.45 W/kg.15 Exposure to nonthermal RF radiation has been reported to influence the electroencephalograms (EEGs) of cats when the field was amplitude-modulated at frequencies less than 25 Hz, which is the range of naturally occurring EEG frequencies.16 The rate of Ca2+ exchange from cat brain tissue in vivo was observed to change in response to similar irradiation conditions.17 Comparable effects on Ca2+ binding were not observed in rat cerebral tissue exposed to RF radiation,18 although the fields used were pulsed at EEG frequencies, rather than

amplitude-modulated. As noted above, the physiological significance of small shifts in Ca2+ binding at nerve cell surfaces is unclear.

A wide variety of changes in brain chemistry and structure have been reported after exposure of animals to high-intensity RF fields.19 The changes include decreased concentrations of epinephrine, norepinephrine, dopamine, and 5-hydroxytryptamine; changes in axonal structure; a decreased number of Purkinje cells; and structural alterations in the hypothalamic region. Those effects have generally been associated with RF intensities that produced substantial local heating in the brain.

Extensive studies have been carried out to detect possible effects of RF radiation on the integrity of the blood-brain barrier.20,21 Although several reports have suggested that nonthermal RF radiation can influence the permeability of the blood-brain barrier, most of the experimental findings indicate that such effects result from local heating in the head in response to SAR values in excess of 2 W/kg. Changes in cerebral blood flow rate, rather than direct changes in permeability to tracer molecules, might also be incorrectly interpreted as changes in the properties of the blood-brain barrier.

Effects of pulsed and sinusoidal ELF fields on the electrical activity of the nervous system have also been studied extensively.22,23 In general, only high-intensity sinusoidal electric fields or rapidly pulsed magnetic fields induce sufficient current density in tissue (around 0.1-1.0 A/m2 or higher) to alter neuronal excitability and synaptic transmission or to produce neuromuscular stimulation. Somewhat lower thresholds have been observed for the induction of visual phosphenes (discussed in the next section) and for influencing the electrical activity of Aplysia pacemaker neurons when the frequency of the applied field matched the endogenous neuronal firing rate.24 Those effects, however, have been observed only with ELF frequencies and would not be expected to occur at the higher frequencies associated with GWEN transmitters. Recent studies with human volunteers exposed to 60-Hz electric and magn.

Electromagnetic radiation can be classified into two types: ionizing radiation and non-ionizing radiation, based on the capability of a single photon with more than 10 eV energy to ionize oxygen or break chemical bonds. Ultraviolet and higher frequencies, such as X-rays or gamma rays are ionizing, and these pose their own special hazards: see radiation and radiation poisoning. By far the most common health hazard of radiation is sunburn, which causes over one million new skin cancers annually.

4.2 Types of hazards

Electrical hazards

Very strong radiation can induce current capable of delivering an electric shock to persons or animals.[citation needed] It can also overload and destroy electrical equipment. The induction of currents by oscillating magnetic fields is also the way in which solar storms disrupt the operation of electrical and electronic systems, causing damage to and even the explosion of power distribution transformers, blackouts (as occurred in 1989), and interference with electromagnetic signals (e.g. radio, TV, and telephone signals).

Fire hazards

Extremely high power electromagnetic radiation can cause electric currents strong enough to create sparks (electrical arcs) when an induced voltage exceeds the breakdown voltage of the surrounding medium (e.g. air at 3.0 MV/m). These sparks can then ignite flammable materials or gases, possibly leading to an explosion.

This can be a particular hazard in the vicinity of explosives or pyrotechnics, since an electrical overload might ignite them. This risk is commonly referred to as

Hazards of Electromagnetic Radiation to Ordnance (HERO) by the United States Navy (USN). United States Military Standard 464A (MIL-STD-464A) mandates assessment of HERO in a system, but USN document OD 30393 provides design principles and practices for controlling electromagnetic hazards to ordnance.

On the other hand, the risk related to fueling is known as Hazards of Electromagnetic Radiation to Fuel (HERF). NAVSEA OP 3565 Vol. 1 could be used to evaluate HERF, which states a maximum power density of 0.09 W/m² for frequencies under 225 MHz (i.e. 4.2 meters for a 40 W emitter)/

Biological hazards

The best understood biological effect of electromagnetic fields is to cause dielectric heating. For example, touching or standing around an antenna while a high-power transmitter is in operation can cause severe burns. These are exactly the kind of burns that would be caused inside a microwave oven.[citation needed]

This heating effect varies with the power and the frequency of the electromagnetic energy, as well as the distance to the source. A measure of the heating effect is the specific absorption rate or SAR, which has units of watts per kilogram (W/kg). The IEEE and many national governments have established safety limits for exposure to various frequencies of electromagnetic energy based on SAR, mainly based on ICNIRP Guidelines, which guard against thermal damage.

There are publications which support the existence of complex biological and neurological effects of weaker non-thermal electromagnetic fields , including weak ELF magnetic fields and modulated RF and microwave fields. Fundamental mechanisms of the interaction between biological material and electromagnetic fields at non-thermal levels are not fully understood.

Lighting.

Fluorescent lights.

Fluorescent light bulbs and tubes internally produce ultraviolet light. Normally this is converted to visible light by the phosphor film inside a protective coating. When the film is cracked by mishandling or faulty manufacturing then UV may escape at levels that could cause sunburn or even skin cancer.

LED lights.

High CRI LED lighting.

Blue light, emitting at wavelengths of 400–500 nanometers, suppresses the production of melatonin produced by the pineal gland. The effect is disruption of a human being's biological clock resulting in poor sleeping and rest periods.

EMR effects on the human body by frequency

Warning sign next to a transmitter with high field strengths

While the most acute exposures to harmful levels of electromagnetic radiation are immediately realized as burns, the health effects due to chronic or occupational exposure may not manifest effects for months or years.[citation needed]

Extremely-low frequency

High-power extremely-low-frequency RF with electric field levels in the low kV/m range are known to induce perceivable currents within the human body that create an annoying tingling sensation. These currents will typically flow to ground through a body contact surface such as the feet, or arc to ground where the body is well insulated.

Shortwave

Shortwave (1.6 to 30 MHz) diathermy heating of human tissue only heats tissues that are good electrical conductors, such as blood vessels and muscle. Adipose tissue (fat) receives little heating by induction fields because an electrical current is not actually going through the tissues.

4.3 Road Transport Safety

The basic strategy of a Safe System approach is to ensure that in the event of a crash, the impact energies remain below the threshold likely to produce either death or serious injury. This threshold will vary from crash scenario to crash scenario, depending upon the level of protection offered to the road users involved. For example, the chances of survival for an unprotected pedestrian hit by a vehicle diminish rapidly at speeds greater than 30 km/h, whereas for a properly restrained motor vehicle occupant the critical impact speed is 50 km/h (for side impact crashes) and 70 km/h (for head-on crashes).

As sustainable solutions for all classes of road have not been identified, particularly low-traffic rural and remote roads, a hierarchy of control should be applied, similar to classifications used to improve occupational safety and health. At the highest level is sustainable prevention of serious injury and death crashes, with sustainable requiring all key result areas to be considered. At the second level is real time risk reduction, which involves providing users at severe risk with a specific warning to enable them to take mitigating action. The third level is about reducing the crash risk which involves applying the road design standards and guidelines (such as from AASHTO), improving driver behavior and enforcement.

4.4 Conclusions

A serious workplace injury or death changes lives forever for families, friends, communities, and coworkers too. Human loss and suffering is

immeasurable. Occupational injuries and illnesses can provoke major crises for the families in which they occur. In addition to major financial burdens, they can impose substantial time demands on uninjured family members. Today, when many families are operating with very little free time, family resources may be stretched to the breaking point. Every person who leaves for work in the morning should expect to return home at night in good health. Can you imagine the knock on the door to tell you your loved one will never be returning home? Or the phone call to say he's in the hospital and may never walk again? Ensuring that husbands return to their wives, wives to their husbands, parents to their children, and friends to their friends that is the most important reason to create a safe and healthy work environment. But it isn't the only reason.

CONCLUSIONS

The work solves the actual problem related to increasing the passive safety of the electric vehicle due to the research and development of the side collision safety system.

As a result of completing the master's thesis, general data on Tesla Model 3 and AUDI E-TRONE electric cars were determined, active and passive safety systems were studied, battery protection measures during a collision were studied, etc. A study of the structure and principle of operation of an asynchronous motor and a battery was carried out.

The calculation of the discharge current of the battery of the Tesla Model S electric car was carried out, which shows that the maximum current through the Panasonic 18650 battery during intensive acceleration of the car can reach a value of 33.8 A, which does not exceed its maximum current according to the technical data. The proposed structure of the mathematical model and the sequence of building the mathematical model based on the scheme of battery replacement during discharge.

Research has been conducted on systems that have the properties of machine vision for the safety system of an electric vehicle. The development of an electric vehicle safety system against a side collision, based on the use of electromagnetic processes occurring in the active electropneumatic suspension of an electric vehicle to reduce the consequences of an accident in the event of a side collision, was carried out.

The issues of labor protection and safety in emergency situations were considered, the safety of electric vehicle protection against short-circuiting of low-voltage and high-voltage batteries was investigated, and an engineering calculation was performed.

REFERENCES

1 2012 Tesla Model S: EPA Range Of 265 Miles, 89 MPGe Efficiency. URL:https://www.greencarreports.com/news/1077122_2012-tesla-model-s-epa-range-of-265-miles-89-mpge-efficiency (date of application 09/27/2021).

2 Tesla 60 kWh Model S Deliveries Delayed To January-February, Entry Level Until March-April. URL: https://insideevs.com/news/316982/tesla-60-kwh-model-s-deliveries-delayed-to-january-february-entry-level-until-march-april/ (application date 09/27/2021).

3 Tesla Kills The Entry-Level, 40 kWh Model S Citing Poor Demand. TechCrunch.2013-04-01. Archive of the original for 2013-04-06. Cited 2021-09-09.

4 Want A 2013 Tesla Model S Signature Edition? Too Late, They're All Gone. Archive of the original for 2013-01-27. Cited 2021-09-09.

5 Tesla Model S turned out to be more popular than German sedans: News: Automobile portal Kolesa.Ru. Archive of the original for June 7, 2013. Cited on September 2, 2021.

6 Electric car Tesla Model S (Obzor AutoArticle.ru) Archived December 7, 2013 inWayback Machine.

7 How we tested Tesla Model S 2016. automoto.ua. Cited 2016-07-21.

8 Vasyura A.S. Electromechanical elements and devices of control systems and automation [Electronic manual] – Vinnytsia. VNTU 2013. – 287 p.

9 Electric machines: teaching. manual for students higher education institutions /L. Ya. Belikova, V. P. Shevchenko. – Odesa.: Nauka i tekhnika, 2012. – 480 p.

10 Control of three-phase engines, methods of speed regulation engines [Electronic resource]: / M. K. Teplov // - Mode of access to the article: http://electricalschool.info/elprivod/1824-upravlenietrekhfaznymi-dvigateljami.html.

11 . Asynchronous electric motors with a phase rotor [Electronic resource]: / Zhukov V. N., Mulych L. I. // - Mode of access to the article: http://electricalschool.info/asinkhronnye-jelektrodvigateli-s-faznym.html

12 Modeling of electromechanical systems. Mathematical modeling of systems asynchronous electric drive: study guide / O. I. Tolochko. - Kyiv, NTUU "KPI", 2016. - 150 p.

13 Tesla Theory Of Operation. http://www.fixyourtesla.com/

14 . M. Blanchard, F.C. Rind, P.F. Verschure. Collision avoidance using a model of the locust LGMD neuron. Robot. Auton. Syst.- 2000. – Vol.30. – P.17-38.

15 . R. Stafford, R.D. Santer, F.C. Rind. A bio-inspired visual collision detection mechanism for cars: combining insect inspired neurons to create a robust system// Biosystems. – 2007.- Vol. 87. - p. 164-171.

16 Honorovsky I.S., Radio schemes and radio signals / I.S. Honorovsky. – M.: Mir, 1981. - 639 p.

17 Ivanov D.Ya. Information exchange in large groups of robots."Artificial Intelligence", No. 4, 2010.

18 Ivanovsky R.I. Visual support of decisions in the SCM environment / R.I. Ivanovsky // Exponenta Pro. Mathematics in applications. - 2006. - #2. -P. 59 - 67.

19 Ivanovsky R.I. Computer technologies in science and education. Practice application of MathCAD Pro systems: учеб allowance / R.I. Ivanovsky. - M.: Higher School, 2003. – 432 p.

20 Engineering handbook of space technologies / [Ed. A.V. Solodova 2nd ed.]. M.: Military Publishing House of the Ministry of Defense of the USSR, 1977.–430 p.

21 Kalyaev I.A., Hayduk A.R., Kapustyan S.G. Models and algorithms of the collective management in groups of robots. Moscow, "Fizmatlit", 2009. - 280 p.

22 . Gurko A.G., Eremenko I.F., Osmachko A.A. /Analysis and synthesis of systems automatic control in MATLAB: Educational and methodological guide. – Kharkiv: Khnadu, 2008. – 284 p.

APPENDIX

APPENDIX A

Conference materials

МІНІСТЕРСТВО ОСВІТИ І НАУКИ УКРАЇНИ
ТЕРНОПІЛЬСЬКИЙ НАЦІОНАЛЬНИЙ ТЕХНІЧНИЙ УНІВЕРСИТЕТ
ІМЕНІ ІВАНА ПУЛЮЯ

М А Т Е Р І А Л И

X НАУКОВО-ТЕХНІЧНОЇ КОНФЕРЕНЦІЇ

«ІНФОРМАЦІЙНІ МОДЕЛІ, СИСТЕМИ ТА ТЕХНОЛОГІЇ»

7–8 грудня 2022 року

ТЕРНОПІЛЬ
2022

УДК 621.317.39:578.087
В. Тимощук, В. Карташов, Р. Королюк, Т. Рубен
(Тернопільський національний технічний університет імені Івана Пулюя, Україна)

ОГЛЯД ПРОТОКОЛІВ КЕРУВАННЯ ДЛЯ ПОБУДОВИ АВТОМАТИЗОВАНИХ СИСТЕМ ВІДДАЛЕНОГО УПРАВЛІННЯ

UDC 621.317.39:578.087
V. Tymoshchuk, V. Kartashov, R. Koroliuk, T. Ruben

OVERVIEW OF CONTROL PROTOCOLS FOR BUILDING AUTOMATED REMOTE CONTROL SYSTEMS

Протокол мережевого обміну інформацією – це перелік типів і форматів переданих блоків даних, правила їх обробки і взаємодії термінальних комп'ютерів на одному рівні. Інтерфейсом називають набір правил, що визначають взаємодію сервісів сусідніх рівнів в одному терміналі.

CoAP – Constrained Application Protocol – це спеціалізований протокол додатків до Інтернету для обмежених пристроїв. Це дозволяє тим обмеженим пристроям, званим «вузлами», спілкуватися з більш широким Інтернетом, використовуючи подібні протоколи. CoAP призначений для використання між пристроями в одній і тій же обмеженій мережі (наприклад, малопотужними, втратними мережами), між пристроями та загальними вузлами в Інтернеті, і між пристроями в різних обмежених мережах, приєднаних до Інтернету. CoAP також використовується за допомогою інших механізмів, таких як SMS у мережах мобільного зв'язку.

Протокол CoAP призначений для взаємодії простих пристроїв, такими як клапани, вимикачі, датчики якими можна керувати або контролювати їхні покази віддалено через мережу Інтернет.

Протокол AMQP: Advanced Message Queuing Protocol Advanced Message Queuing Protocol (AMQP) – це відкритий протокол, для передачі повідомлень між компонентами системи з низькою затримкою і на досить високій швидкості. AMQP може налаштовується під потреби конкретного проекту і передбачає надійний транспортний протокол, такий як TCP.

Ідея цього протоколу полягає в обміні довільним чином повідомленнями через AMQP-брокер, який здійснює маршрутизацію, гарантує доставку, розподіл потоків даних, підписку на потрібні типи повідомлень.

Головною перевагою AMQP є функція зберігання, а також передачі даних, яка забезпечує надійність навіть якщо в роботі мережі стався збій. Недоліком протоколу AMQP є низький рівень успішності доставки при низькій пропускній здатності та збільшується при збільшенні пропускної здатності. А перевагою, порівнюючи AMQP з REST, протокол AMQP може відправляти більшу кількість повідомлень у секунду.

MQTT або Message Queue Telemetry Transport – це легкий, компактний і відкритий протокол обміну даними створений для передачі даних на віддалених локаціях, де потрібно невеликий розмір коду і є обмеження по пропускній здатності каналу.

Також існує версія протоколу MQTT-SN (MQTT for Sensor Networks), раніше відома як MQTT-S, яка призначена для вбудованих бездротових пристроїв без підтримки TCP / IP мереж, наприклад, Zigbee.

Основними особливостями протоколу повідомлень MQTT є:

- асинхронний протокол
- компактні повідомлення
- Робота в умовах нестабільного зв'язку на лінії передачі даних
- Підтримка декількох рівнів якості обслуговування (QoS)
- Легка інтеграція нових пристроїв

Протокол MQTT працює на прикладному рівні поверх TCP/IP і використовує за замовчуванням 1883 порт.

Обмін повідомленнями в протоколі MQTT здійснюється між клієнтом (client), який може бути видавцем або підписником (publisher/subscriber) повідомлень, і брокером (broker) повідомлень (наприклад, Mosquitto MQTT).

Видавець відправляє дані на MQTT брокер, вказуючи в повідомленні певну тему, топік (topic). Підписники можуть отримувати різні дані від безлічі видавців залежно від підписки на відповідні топіки.

Пристрої MQTT використовують певні типи повідомлень для взаємодії з брокером, нижче представлені основні:

Connect – встановити з'єднання з брокером
Disconnect – розірвати з'єднання з брокером
Publish – опублікувати дані в топік на брокера
Subscribe – підписатися на топік на брокера
Unsubscribe – відписатися від топіка

Схему взаємодії між підписником, видавцем і брокером можна переглянути на рисунку 1.

Рисунок 1. Схема взаємодії між підписником, видавцем і брокером

Видавець відправляє дані на MQTT брокер, вказуючи в повідомленні певну тему, топік (topic). Підписники можуть отримувати різні дані від безлічі видавців залежно від підписки на відповідні топіки.

Аналізуючи всі три види протоколів для використання їх для розробки навчальним стендів віддаленого керування на нашу думку необхідно обрати протокол MQTT, як найбільш гнучкий в даному плані.

Література

1. Що таке MQTT і для чого він потрібет в IIoT? Опис протоколу MQTT. URL: http://edu.asu.in.ua/mod/book/tool/print/index.php?id =116.
2. Протокол обмеженого застосування. URL: https://en.wikipedia.org/wiki/Constrained_Application_Protocol.
3. Сервоприводи. URL: http://www.princeton.edu/~mae412/TEXT/NTRAK2002/292-302.pdf.
4. Ардуіно. URL: https://uk.wikipedia.org/wiki/Arduino.

МІНІСТЕРСТВО ОСВІТИ І НАУКИ УКРАЇНИ
Тернопільський національний технічний університет імені Івана Пулюя (Україна)
Університет імені П'єра і Марії Кюрі (Франція)
Маріборський університет (Словенія)
Технічний університет у Кошице (Словаччина)
Вільнюський технічний університет ім. Гедимінаса (Литва)
Міжнародний університет цивільної авіації (Марокко)
Наукове товариство ім. Т.Шевченка

АКТУАЛЬНІ ЗАДАЧІ СУЧАСНИХ ТЕХНОЛОГІЙ

Збірник
тез доповідей

XI Міжнародної науково-практичної конференції молодих учених та студентів
7-8 грудня 2022 року

УКРАЇНА
ТЕРНОПІЛЬ – 2022

Матеріали XI Міжнародної науково-практичної конференції молодих учених та студентів «АКТУАЛЬНІ ЗАДАЧІ СУЧАСНИХ ТЕХНОЛОГІЙ» – Тернопіль, 7-8 грудня 2022 року

УДК 629.762

М.С. Дзюмак, Р.З. Золотий, к.т.н., доцент, О.С. Голотенко, к.т.н., доцент, Т.Е.Рубен
Тернопільський національний технічний університет імені Івана Пулюя, Україна

МОДЕЛЮВАННЯ РУХУ ТРАНСПОРТУЮЧОЇ СИСТЕМИ ЗАЛЕЖНО ВІД НАЯВНИХ ПЕРЕШКОД

M.S. Dziumak, R.Z. Zolotyi, Ph.D., Assoc. Prof., O.S. Holotenko, Ph.D., Assoc. Prof., T.E. Ruben

SIMULATION OF THE MOVEMENT OF THE TRANSPORTATION SYSTEM DEPENDING ON PRESENT OBSTACLES

Зі стрімким розвитком комп'ютерів, електроніки та сенсорних технологій настала ера штучного інтелекту. Розумний транспортний засіб може частково або повністю замінити людину для виконання завдань водіння, транспортування, що має велике значення для підвищення безпеки дорожнього руху та ефективності транспортування. Однак складні сценарії водіння все ще є складними для інтелектуальних транспортних засобів, наприклад, сусідні транспортні засоби на суміжних смугах руху перерізають траєкторію транспортного засобу. Коли поруч з'являється перешкода, інтелектуальний транспортний засіб має не лише слідувати своїй власній орієнтовній траєкторії, а й реагувати на перешкоду, наприклад виконувати екстрене гальмування, щоб забезпечити безпеку між сусіднім транспортним засобом і транспортним засобом.

Щоб гарантувати, що інтелектуальний транспортний засіб завжди підтримує безперебійний процес керування, намір автомобіля, що знаходиться поруч, має бути розпізнано заздалегідь, і його прогнозована траєкторія стає частиною еталону для планування траєкторії транспортного засобу.

Метою роботи було запропонувати метод керування відстеженням траєкторії, заснований на прогнозуванні поведінки врізання. Застосовується метод розпізнавання наміру в'їзду, щоб оцінити можливість сусіднього транспортного засобу, а модель попереднього перегляду водія використовується для прогнозування траєкторії врізаного автомобіля.

Було використано три сценарії водіння розділені для керування плануванням траєкторії за різних режимів врізання. Результати моделювання приведені на рис. 1.

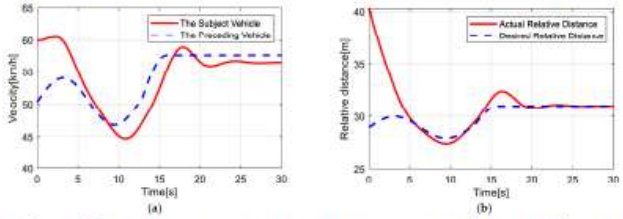

Рисунок 1 - Результати моделювання сценарію водіння: (a) швидкість досліджуваного транспортного засобу та транспортного засобу, що врізався; (b) відносна відстань між транспортними засобами.

Література.

1. Yang, J.; Coughlin, J.F. In-vehicle technology for self-driving cars: Advantages and challenges for aging drivers. Int. J. Automot. Technol. **2014**, 15, 333–340.
2. Trajectory Tracking Control for Intelligent Vehicles Based on Cut-In Behavior Prediction / Chongpu Chen,Jianhua Guo,Chong Guo,Xiaohan Li andChaoyi Chen // Electronics 2021, 10(23), 2932.